Atmos. Chem. Phys., 25, 4107–4129, 2025
https://doi.org/10.5194/acp-25-4107-2025

Atmospheric Chemistry and Physics
Open Access
EGU

Research article

Marine organic aerosol at Mace Head: effects from phytoplankton and source region variability

Emmanuel Chevassus[1], Kirsten N. Fossum[1], Darius Ceburnis[1], Lu Lei[1], Chunshui Lin[1,2], Wei Xu[1,a], Colin O'Dowd[1], and Jurgita Ovadnevaite[1]

[1]School of Natural Sciences, Centre for Climate & Air Pollution Studies, Ryan Institute, University of Galway, Galway, Ireland
[2]Institute of Urban Environment, Chinese Academy of Sciences, Xiamen 361021, China
[a]now at: State Key Laboratory of Loess and Quaternary Geology (SKLLQG), Center for Excellence in Quaternary Science and Global Change, Institute of Earth Environment, Chinese Academy of Sciences, Xi'an 710061, China

Correspondence: Jurgita Ovadnevaite (jurgita.ovadnevaite@universityofgalway.ie)

Received: 16 September 2024 – Discussion started: 24 September 2024
Revised: 24 January 2025 – Accepted: 27 January 2025 – Published: 10 April 2025

Abstract. Organic aerosol (OA) is recognized as a significant component of particulate matter (PM), yet their specific composition and sources, especially over remote areas, remain elusive due to the overall scarcity of high-resolution online data. In this study, positive matrix factorization was performed on organic aerosol mass spectra obtained from high-resolution time-of-flight aerosol mass spectrometer (HR-ToF-AMS) measurements to resolve sources contributing to coastal PM. The focus was on a summertime period marked by enhanced biological productivity with prevailing pristine maritime conditions. Four OA factors were deconvolved by the source apportionment model. The analysis revealed primary marine organic aerosol (PMOA) as the predominant submicron OA at Mace Head during summertime, accounting for 42 % of the total resolved mass. This was trailed by more oxidized oxygenated organic aerosol (MO-OOA) at 32 %, methanesulfonic acid organic aerosol (MSA-OA) at 17 %, and locally emitted peat-derived organic aerosol (peat-OA) at 9 % of the total OA mass. Elemental ratios (O : C–H : C) were derived for each of these factors: PMOA (0.66–1.16), MO-OOA (0.78–1.39), MSA-OA (0.66–1.39), and peat-OA (0.43–1.34). The specific O : C–H : C range for MO-OOA hints at aliphatic and lignin-like compounds contributing to more oxidized organic aerosol formation. The total mass concentrations of primary organic aerosol and secondary organic aerosol were overall equal and almost exclusively present in the marine boundary layer, in agreement with previous findings. This study reveals that OA not only reflects atmospheric chemistry and meteorology – as evidenced by the significant ageing of summertime polar air masses over the North Atlantic, driven by ozonolysis under Greenland anticyclonic conditions – but also serves as an indicator of marine ecosystems. This is evident from MSA-OA being notably associated with stress enzyme markers and PMOA showing the typical makeup of largely abacterial phytoplankton extracellular metabolic processes. This study also reveals distinct source regions within the North Atlantic for OA factors. MSA-OA is primarily associated with the Iceland Basin, with rapid production following coccolithophore blooms (lag of 1–2 d), while diatoms contribute to a slower formation process (lag of 9 d), reflecting distinct oceanic biological processes. In contrast, PMOA is sourced from more variable ecoregions, including the southern Celtic Sea, western European Basin, and Newfoundland Basin, with additional contributions from chlorophytes and cyanobacteria at more southerly latitudes. Overall, these findings emphasize the need for longer-term investigations to further map the influence of phytoplankton taxa variability on aerosol composition and the broader impacts on aerosol–climate interactions.

Published by Copernicus Publications on behalf of the European Geosciences Union.

1 Introduction

The marine environment plays a critical role in climate regulation through sea spray and gas-phase emissions from the oceans, via direct and indirect solar radiation effects and aerosol–cloud interactions governed by ocean biology, sea spray physicochemical properties, and secondary reactions (Cochran et al., 2017). Aerosol in the atmospheric marine boundary layer (MBL) remains a significant source of uncertainty in radiative forcing estimates (Rosenfeld et al., 2019; Wang et al., 2020), primarily due to limited knowledge about aerosol mass, chemical composition, and particle number distributions (Carslaw et al., 2017). Radiative transfer implications from aerosol–cloud interactions alone range from -2.65 to $-0.07\,\mathrm{W\,m^{-2}}$, contrasting with the more well-established CO_2 radiative forcing estimate of $1.83 \pm 0.18\,\mathrm{W\,m^{-2}}$ (Etminan et al., 2016). Along with this, the origin of marine organic aerosol (OA), specifically whether formed by primary or secondary processes, requires further investigation, as the respective impacts from primary sea spray (Fossum et al., 2018; Ovadnevaite et al., 2011; Xu et al., 2021) and secondary aerosol (Mayer et al., 2020; Quinn et al., 2017) on cloud formation or atmosphere optical properties (Bian et al., 2019; Kahnert and Kanngießer, 2023; Li et al., 2023) in pristine environments is still being debated.

Primary marine organic aerosol (PMOA) is part of sea spray aerosol, produced by wave breaking (Ovadnevaite et al., 2014; Veron, 2015; Villermaux et al., 2022) and made of biogenic organic matter (O'Dowd et al., 2004; Facchini et al., 2008). The majority (80 %) of fine carbonaceous particles in the clean northeastern Atlantic marine atmosphere have been shown to directly originate from phytoplankton activity as reported with dual-carbon isotope analysis (Ceburnis et al., 2011). The phytoplankton–OA link is particularly well-established, yet the topic is still highly debated as no clear full-picture consensus has been reached owing to widely changing temporal and geographic fluctuations (Lawler et al., 2024; Lewis et al., 2021; Seidel et al., 2022). In addition, the specifics of how phytoplankton control OA chemical composition (Behrenfeld et al., 2019; Facchini et al., 2008; O'Dowd et al., 2015), particle number flux (Markuszewski et al., 2024; Sellegri et al., 2023), size (Croft et al., 2021; O'Dowd et al., 2004; Saliba et al., 2019), lifespan, and surface tension (Lee et al., 2020; Ovadnevaite et al., 2017; Sellegri et al., 2021) are all the focus of intense ongoing investigations.

In a warming world, following a high-emissions scenario (RCP8.5, Representative Concentration Pathway) trajectory, climate change is projected to drastically alter the geographic and seasonal variability of phytoplankton blooms in the northeastern Atlantic (Asch et al., 2019). Furthermore, long-term trends already show that the northeastern Atlantic has experienced major changes in phytoplankton functional diversity over the last 60 years (i.e. -5 % dinoflagellates per decade vs. $+0.1$ % diatoms per decade) due to rapid warming and various environmental transformations attributable to climate change (Bedford et al., 2020; Holland et al., 2023; Mutshinda et al., 2024). All of this strongly supports the pressing needs for further investigations on phytoplankton–aerosol interactions as environmental stressors will result in significant non-linear effects and tipping points (Ban et al., 2022; Wolf et al., 2024).

In contrast to PMOA, marine secondary organic aerosol (SOA) in the remote MBL arises from new particle formation (NPF) and is governed by other subtle chemical mechanisms. These include gas-to-particle conversion (Peltola et al., 2022; Zheng et al., 2021), oxidation of volatile organic compounds and consequent volatility reduction that leads to condensation (Hallquist et al., 2009; Kroll et al., 2018), ion-induced nucleation of biogenic particles (Kirkby et al., 2016), and fission of organic biogels (Karl et al., 2013). SOA formation occurs through various processes such as homogeneous, heterogeneous, and multiple-phase reactions (Marais et al., 2016; McNeill, 2015) as well photochemistry reactions (Brüggemann et al., 2018). While various SOA molecular classes have been identified, the complexity of SOA, which consists of thousands of multifunctional compounds (Goldstein and Galbally, 2007), including high-molecular-weight species and oligomers from diverse sources, underscores the pressing need for continued exploration. All of this can now be partly described thanks to continuous widespread progress in aerosol mass spectrometry (DeCarlo et al., 2006; Laskin et al., 2012).

The present study focuses on source apportionment in a coastal environment, with the aim to separate primary OA (POA) and SOA into their respective sources. Marine SOA sources notably include methanesulfonic acid that is formed through the oxidation of dimethyl sulfide (Becagli et al., 2019; Hodshire et al., 2019; Mansour et al., 2024) and oxidized OA (i.e. carboxylic acids; Kawamura and Bikkina, 2016) that are complex mixtures resulting from unsaturated fatty acid oxidation found in very diverse locations (Crippa et al., 2013; Florou et al., 2024; Nøjgaard et al., 2022). On the other hand, POA sources not only include sea spray but also potential anthropogenic influences like local biomass burning (i.e. wood, peat, or charcoal) or long-range continental transport (Lin et al., 2019; O'Dowd et al., 2014; Xu et al., 2020). The source apportionment was performed with the positive matrix factorization (PMF) model which has been widely adopted for more than 2 decades now (Paatero, 1999; Paatero and Tapper, 1994) and successfully used on a wide range of different instruments: an HR-ToF-AMS (high-resolution time-of-flight aerosol mass spectrometer; e.g. Aiken et al., 2008), a ToF-ACSM (time-of-flight aerosol chemical speciation monitor; e.g. Fröhlich et al., 2015), a PTR-MS (proton transfer reaction mass spectrometer; e.g. Slowik et al., 2010), an EESI-ToF (extractive electrospray ionization time-of-flight mass spectrometer; e.g. Tong et al., 2022), offline filters (e.g. Maykut et al., 2003), and an SMPS (scanning mobility particle sizer; e.g. Nursanto et al.,

2023) as well as other matrix-based measurements. Several previous remote-ocean HR-ToF-AM PMF studies have been carried out in the Atlantic (Crippa et al., 2013; Huang et al., 2018), the Arctic (Moschos et al., 2022; Nielsen et al., 2019; Nøjgaard et al., 2022), the Mediterranean Sea (Florou et al., 2024; Mallet et al., 2019), the Pacific (Loh et al., 2023, 2024), and Antarctica (Giordano et al., 2016; Paglione et al., 2024; Schmale et al., 2013), facilitating cross-site comparability.

This study seeks to relate different aerosol sources and geographical regions to phytoplankton taxonomic-group simulations (Rousseaux et al., 2013), as the effects from ocean biology are not unaccounted for in current climate models (Sellegri et al., 2021). This multi-faceted approach places the local measurements at Mace Head into the broader context of ocean–atmosphere interactions, allowing for the exploration of the potential influences of marine ecosystems on atmospheric aerosol over the North Atlantic region.

2 Materials and methods

2.1 Site description

The Mace Head (MHD) Atmospheric Research Station is located on the western coast of Ireland (53.33° N, 9.90° W) on a peninsula exposed to open-ocean air masses. These air masses, originating from a nominally clean sector (between 190 and 300°; Grigas et al., 2017), are predominantly steered by westerlies ushered by the polar jet's low-pressure systems. Importantly, open-ocean air masses are mostly devoid of anthropogenic influences, with over 60 % of air masses arriving at MHD classified as pristine marine (Grigas et al., 2017; Sanchez et al., 2022). However, the remaining 40 % of all the other air masses exhibit varying degrees of anthropogenic influences, particularly during or just after periods of continental outflow under high-pressure regimes (Jennings et al., 2003).

This study focuses on August 2015, a summertime period characterized by heightened biological activity (Behrenfeld et al., 2019) and predominantly pristine-marine conditions. This specific year is also marked by the onset of the *cold blob*, with the subpolar-gyre region (North Atlantic waters south of Greenland) reaching around 2 °C lower than the previous long-term average, possibly owing to the slowing down of the Atlantic meridional circulation and Greenland ice melt (Rahmstorf et al., 2015; Sanders et al., 2022). As such these specific conditions could serve as an indication for future measurements of aerosol–phytoplankton interactions during cold-blob phenomena.

2.2 In situ measurements

Aerosol chemical composition was monitored using an Aerodyne high-resolution time-of-flight aerosol mass spectrometer (HR-ToF-AMS) equipped with a standard tungsten vaporizer operated at 650 °C. HR-ToF-AMS sampling covers the vacuum aerodynamic size range of ∼35 to ∼1.5 µm (DeCarlo et al., 2006). The instrument working principles have been extensively described in the literature (Canagaratna et al., 2007; DeCarlo et al., 2006). The HR-ToF-AMS used a 5 min time resolution scan on the single-reflection highly sensitive V mode configuration (mass resolution up to 3000 m Δm^{-1}), while detection limits were estimated based on the approach described by Drewnick et al. (2009). Ionization efficiency (IE), particle velocity, and inlet flow were determined following standard methods while applying standard relative IE (RIE) for species (Nault et al., 2023; Xu et al., 2018). The particle transmission and detection efficiency expressed as the collection efficiency (CE; Huffman et al., 2005) was corrected for detection losses due to particle bounce and lens efficiency by applying the composition-dependent collection efficiency (Middlebrook et al., 2012).

The AMS data were analysed using the SQUIRREL (SeQUential Igor data RetRiEvaL) v1.65B and PIKA (Peak Integration by Key Analysis) v1.25B software packages. Sea salt was estimated based on a scaling factor of 51 of the common sea salt ion $NaCl^+$ (m/z 57.96) (Ovadnevaite et al., 2012), while MSA was quantified by upscaling the CH_3SO_2 (m/z 79) ion (Ovadnevaite et al., 2014). Interferences from MSA on SO_4 and OA were accounted for as follows:

$$SO_{4\ \mathrm{corrected}} = SO_4 - \frac{CH_3SO_2 \times 12.48}{RIE_{SO_4}},$$

$$OA_{\mathrm{corrected}} = OA - \frac{CH_3SO_2 \times 15.86}{RIE_{\mathrm{Orgs}}}.$$

An improved-ambient (I-A) method was adopted for the mass spectra elemental-ratio analysis of O : C, H : C, N : C, S : C, and OM : OC (organic matter to organic carbon) (Canagaratna et al., 2015). High-resolution analysis was performed on each m/z in the mass range 12–130 m/z with ion fitting applied to difference between open and closed spectra. Based on their elemental composition (C, O, H, N, S), ions were then grouped into chemical families: C_x, C_xH_y, $C_xH_yO_z$ ($z = 1$), $C_xH_yO_z$ ($z > 1$), $C_xH_yN_w$ ($w = 1$), $C_xH_yN_w$ ($w > 1$), C_xS_j, H_yO_z, N_wH_y, N_wO_z, S_jO_z, and C_xS_i, where the indices x, y, z, w, and j represent the number of C, H, O, N, and S atoms, respectively.

The concentration of equivalent black carbon (eBC) was measured by a multiangle absorption photometer (MAAP; Thermo Fisher Scientific model 5012). The MAAP operated at a flow rate of 10 L min^{-1} and a 5 min time resolution. The transmittance and reflectance of eBC-containing particles were measured by the MAAP at two different angles to derive optical absorbance as detailed in Xu et al. (2020).

Carbon monoxide (CO) measurements were also conducted using a model RGA-3 CO analyser (Trace Analytical, Inc., CA, USA), which operates on the principle of hot mercuric oxide reduction gas chromatography (Derwent et al., 1994).

Ozone (O_3) was measured at the station with a UV O_3 spectrometer (model 8810, Monitor Labs, San Diego, CA); the raw voltage output was converted to concentration values based on Automatic Urban and Rural Network (AURN) calibration audits (Derwent et al., 2018). Finally, meteorological data were continuously recorded at the station (including rainfall, irradiance, wind speed, wind direction, temperature, relative humidity, and pressure) using standard meteorological instruments and retrieved using the R package `worldmet` (station ID: 039630-99999) from the NOAA Integrated Surface Database (ISD) website (https://www.ncdc.noaa.gov/isd, last access: 14 December 2023).

2.3 Source apportionment

The HR organic mass spectra was deconvolved using the positive matrix factorization (PMF; Paatero and Tapper, 1994; Paatero, 1999) source–receptor model to investigate the various source contributions to OA. A major advantage of using HR data over unit mass resolution (i.e. ToF-ACSM studies) is the distinct differentiation of multiple ions sharing the same nominal mass, thereby allowing for a more exact characterization of the temporal fluctuations of different ion families (e.g. $C_xH_y^+$, $C_xH_yO_z^+$). The information richness in the HR-ToF-AMS datasets, as a result of the improved chemical resolution, is advantageous for restricting the PMF solutions, minimizing rotational ambiguity and resulting in more reliable solutions and a larger number of interpretable OA factors.

The Igor Pro Source Finder (SoFi v6.8.1) toolkit (Canonaco et al., 2013) was used to run the PMF algorithm. Solutions were assessed across 2 to 12 factors using the unconstrained-factor rotational Fpeak tool. Factors were explored for Fpeaks (rotations) between -1 and 1 (0.1 steps). A final solution consisting of four factors was retained as the optimal solution based on several considerations. These include its ratio of observed and expected residuals, ensuring an optimal fit (Q/Qexp value of 1.38), which is tested for a range of Fpeaks and scaled-residual distributions (as recommended by Zhang et al., 2011). The solutions were also investigated in regard to key diagnostic plots, diurnal profiles, correlations with meaningful external tracer time series, and reference mass spectra (Canonaco et al., 2021) extracted from the aerosol mass spectrometer database (Ulbrich et al., 2009).

2.4 Air mass trajectory analysis

Air mass back trajectory analysis was performed using the Hybrid Single-Particle Lagrangian Integrated Trajectory (HYSPLIT) (Stein et al., 2015). Meteorological data were accessed from the Global Data Assimilation System (GDAS) archived by the NOAA Air Resources Laboratory. HYSPLIT was used to calculate 72 h back trajectories every 3 h with the arrival height set to 100 m above ground level. To investigate potential source regions leading to total particle mass concentrations from each resolved source, the back trajectories were gridded to $1° \times 1°$ grid cells and linked to particle concentrations using trajectory source contribution functions. While common source contribution functions assume that trajectory centrelines are accurate, we focused instead on the simplified quantitative transport bias analysis (STQBA) method which considers plume transport bias along air mass trajectories as a more robust approach.

The boundary layer height (BLH) was determined from the fifth-generation ECMWF (European Centre for Medium-Range Weather Forecasts) atmospheric reanalysis (ERA5) dataset based on the bulk Richardson number (Guo et al., 2021) by mapping the HYSPLIT trajectory footprint along the gridded BLH data. This was used to find the fraction of time spent over the ocean, within the marine boundary layer (MBL; altitude < BLH), in the marine free troposphere (MFT; altitude > BLH), and in the planetary boundary layer (PBL) over land (altitude < BLH). The R package `rnaturalearth` was also used to obtain a high-resolution land mask for Ireland, allowing for identification of purely marine air masses (no advection over land for at least 3 d prior to being sampled at MHD) and aiding in delineating land from ocean.

Finally, NASA Ocean Biogeochemical Model (NOBM) taxonomic-group simulations (Rousseaux et al., 2013) for coccolithophores, diatoms, chlorophytes, and cyanobacteria were used to visualize phytoplankton geographic repartition estimates as well as for lag calculations with OA similarly to O'Dowd et al. (2015).

2.5 Transfer entropy analysis

The R package `RTransferEntropy` (Behrendt et al., 2019) was used to quantify the information flow between time series using the transfer entropy (TE) as previously done in recent SOA studies (Long et al., 2023; Sinha et al., 2024). Transfer entropy (TE) is a prediction model that quantifies the directional influence between two time series X and Y by determining how the past values of one series predict the future behaviour of the other (Schreiber, 2000). TE is calculated using Rényi entropy, a generalization of Shannon entropy that offers enhanced robustness in the presence of tail effects. To account for spurious information transfer, the transfer entropy is also estimated from a shuffled version of the time series. This shuffled estimate called effective transfer entropy (eTE) is used to correct for sampling bias, ensuring the validity of the results. Statistical significance is assessed with a bootstrapped Markov chain, where a p value of less than 0.05 indicates a significant information transfer between X and Y. The reader is referred back to Behrendt et al. (2019) for more details.

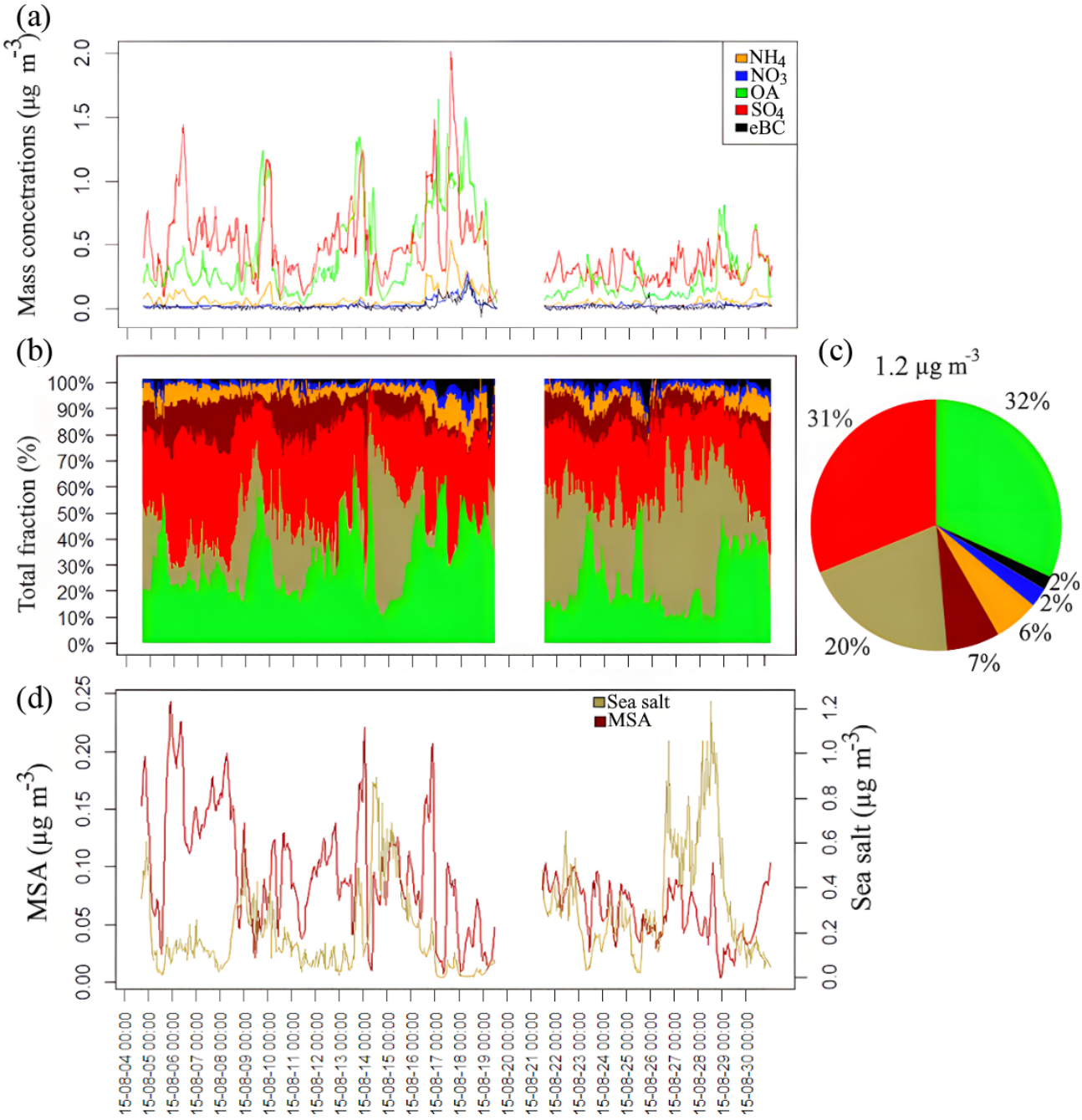

Figure 1. **(a)** OA, SO_4, NH_4, NO_3, and eBC mass concentration time series ($\mu g\,m^{-3}$). **(b)** Relative contributions to total PM_1. **(c)** Pie plot of total contributions to total PM_1. **(d)** MSA and sea salt ($\mu g\,m^{-3}$).

3 Results

3.1 Submicron aerosol chemical composition overview

The mass concentration time series of organic aerosol (OA), methanesulfonic acid (MSA), sulfate (SO_4^{2-}), nitrate (NO_3^-), ammonium (NH_4^+), and sea salt measured by the HR-ToF-AMS as well as eBC from MAAP measurements are shown in Fig. 1. The average chemical composition was dominated by OA (32 %), followed by SO_4^{2-} (31 %), sea salt (20 %), MSA (7 %), NH_4^+ (6 %), NO_3^- (2 %), and eBC (2 %) (Fig. 1).

The total average bulk submicron aerosol mass was 1.2 $\mu g\,m^{-3}$ over the entire measurement period. These high SO_4^{2-} and OA relative contributions and overall low concentrations are common for coastal sites during summertime in the marine boundary layer as reported over the North and South Atlantic (Huang et al., 2018; Ovadnevaite et al., 2014)

as well as in the Arctic (Nielsen et al., 2019; Willis et al., 2017). MSA in particular showed mass concentration values of $0.08 \pm 0.04\,\mu g\,m^{-3}$ in the range of those previously reported at Mace Head (0.05 ± 0.04) (Ovadnevaite et al., 2011) and more diverse locations such as the central Arctic (Dada et al., 2022) and the Atlantic Ocean from 53° N to 53° S, where average mass concentrations of $0.04 \pm 0.03\,\mu g\,m^{-3}$ (Huang et al., 2018) were reported.

The low mass concentrations of NH_4^+ and NO_3^- and corresponding N : C ratio of 0.006 ± 0.002 (Fig. S1 in the Supplement) indicate a limited presence of amino acids (below the detection limit) from the usual sources such as the North Atlantic oligotrophic gyre, ornithogenic emissions (i.e. birds), phytoplankton, bacteria, or in situ atmospheric processes (van Pinxteren et al., 2022; Schmale et al., 2013).

Following eBC thresholds established for the northeastern Atlantic (Grigas et al., 2017), pristine conditions (eBC levels below $0.015\,\mu g\,m^{-3}$) were observed during 60.4 % of the measurement period. Clean conditions (eBC levels between 0.015 and $0.05\,\mu g\,m^{-3}$) prevailed for 30.5 % of the time, and moderately polluted conditions (eBC levels between 0.05 and $0.3\,\mu g\,m^{-3}$) occurred for 9.1 % of the time, with a significant pollution event spanning from 17 to 19 August 2015 onwards.

Likewise, CO mixing ratios were below 100 ppb for over 70 % of the time, similarly to other pristine sites (Zhao et al., 2022). Winds advected through the clean sector (190–300°) for over 78 % of the time. Finally the mean wind speed was $6.6 \pm 3.1\,m\,s^{-1}$, exceeding the whitecap threshold of $4\,m\,s^{-1}$ (O'Dowd et al., 2014) for 77 % of the time, hinting at strong sea spray influences.

There were also SOA influences indicated by the average ratio value of OM : OC (organic matter to organic carbon) of 2.10 ± 0.14 (Fig. S1), aligning with the value of 1.9 previously reported for clean aged marine polar air masses at MHD (Ovadnevaite et al., 2014). Additionally, AMS-derived OM : OC values in the high Arctic (Nielsen et al., 2019) also fall within the range of 1.96 to 2.42 for PMOA (primary marine organic aerosol) and MO-OOA (more oxidized oxygenated organic aerosol), respectively, where the median OM : OC value was 2.11 with minimum and maximum OM : OC values of 1.71 and 2.42, respectively. This indicates the presence of both POA (i.e. saturated hydrocarbons, unsaturated hydrocarbons, and cycloalkanes) as well as oxygenated SOA formed with photochemical processing during long-range transport (Aiken et al., 2008; Simon et al., 2011).

To get a better sense of the aerosol sources, the respective contributions of the marine boundary layer (MBL), marine free troposphere (MFT), and boundary layer (BL) over land are shown in Fig. S2 in the Supplement. Overall, the measurement period was dominated by marine boundary layer influences (91 % of the time), with minimal influences from the marine free troposphere (8 %) and extremely low land influences from the planetary boundary layer (1 %), further evidencing pristine-marine conditions.

3.2 Source apportionment

To accurately classify and categorize the diverse sources of OA that are present at Mace Head, source apportionment was performed utilizing the positive matrix factorization (PMF) method on the organic mass spectrum, which ranged from m/z 12 to m/z 130. The resulting chosen four-factor solution, as depicted in Fig. 2, yielded a Q/Qexp ratio of 1.38 and accounted for up to 90 % of the total OA mass. Solutions with a higher number of factors introduced splitting and did not show additional emergent interpretable sources (Fig. S3, Sect. S1 in the Supplement).

The following four factors, namely methanesulfonic acid, more oxidized organics, primary marine organics, and peat, were determined as the optimal representation of aerosol at Mace Head.

Methanesulfonic acid organic aerosol (MSA-OA), representing approximately 17.2 % of the total OA mass, displayed a distinct m/z fragment at m/z 78.98 ($CH_3SO_2^+$), accounting for 36.3 % of its total mass spectra signal intensity. The identification of specific methane sulfonic acid tracer ions further substantiated its origin. More details on all factors are provided below in Sects. 3.2.1–3.2.4.

More oxidized organic aerosol (MO-OOA), making up about 31.8 % of the total elucidated PMF solutions, exhibited prominent m/z fragments at m/z 27.99 and m/z 43.99 and showed significant correlations with reference mass spectra for MO-OOA ($R = 0.97$) (Hu et al., 2015) and SV-OOA (semi-volatile; $R = 0.76$) (Mohr et al., 2012) and was interpreted as MO-OOA after examining elemental ratios and correlations.

Primary marine organic aerosol (PMOA) comprises roughly 42.2 % of the total resolved PMF solutions. This factor exhibited m/z fragments similar to those of MO-OOA (Schmale et al., 2013) but with higher contributions from aliphatics (C_xH_y) such as alkyls (dominant in sea spray during phytoplankton blooms; Cavalli, 2004), alkenes (i.e. phenols or humic materials; Bahadur et al., 2010), and functional derivatives such as alcohols ($C_xH_yO_z$, where $z = 1$) as established in earlier studies (Ovadnevaite et al., 2011; Crippa et al., 2013).

Peat-OA, accounting for approximately 8.8 % of the total PMF solutions, was characterized by ion series of saturated hydrocarbons (C_xH_{2y+1}), unsaturated hydrocarbons (C_xH_{2y-1}), and cycloalkanes (C_xH_{2y}). This factor was identified as peat-OA owing to its good correlation ($R = 0.75$) with the peat-OA reference mass spectra (Lin et al., 2017). Additionally, its mass spectrum was marked by cellulose pyrolysis fragments typical of levoglucosan (i.e. $C_2H_4O_2^+$ at m/z 60 and $C_3H_5O_2^+$ at m/z 73) and by the dominance of $C_3H_7^+$ rather than $C_2H_3O^+$ at m/z 43, which facilitated the distinction of peat emissions over wood or smoky coal emissions.

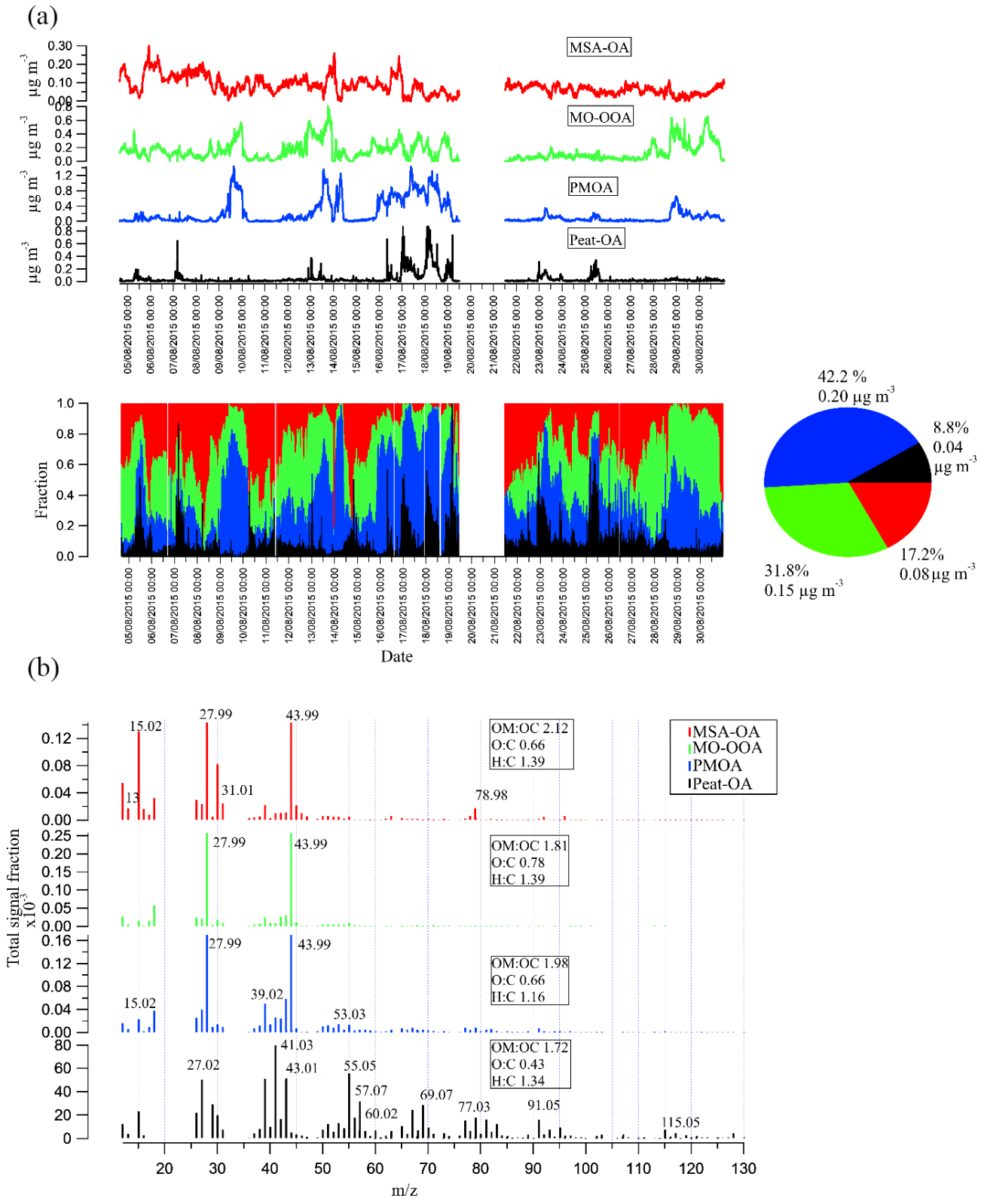

Figure 2. **(a)** Factor time series (MSA-OA in red, MO-OOA in green, PMOA in blue, peat-OA in black) and associated relative-contribution time series and pie chart showing fractions and respective mass concentrations ($\mu g\,m^{-3}$) for the whole period. **(b)** Factor mass spectra (MSA-OA in red, MO-OOA in green, PMOA in blue, peat-OA in black) and associated improved ambient OM : OC, O : C, and H : C ratios (Canagaratna et al., 2015).

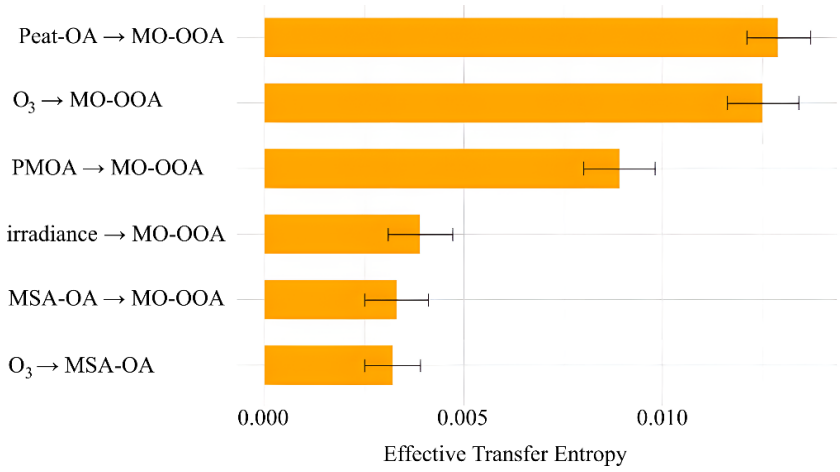

Figure 3. Significant ($p = 0$) flow values of effective transfer entropy between PMF factors, ozone, and irradiance.

3.2.1 More oxidized oxygenated organic aerosol (MO-OOA)

MO-OOA main contributing ions are associated with oxygenated compounds belonging to the COOH functional group (Fig. S5 in the Supplement), reflecting pronounced fragmentation of mono- and dicarboxylic acids into fragments with multiple oxygen atoms (Duplissy et al., 2011). Specifically, the $C_xH_yO_z$ ($z > 1$) ion family accounts for 63.1 % of the total mass spectra intensity, followed by the $C_xH_yO_z$ ($z = 1$) ion family (m/z 27.99, m/z 43.02, m/z 42.01, etc.) contributing 13.68 % to MO-OOA, adding up to a total contribution of 76.8 %. Additionally, CO^+ and CO_2^+ account for 25 % of MO-OOA intensity, which is typical of remote-ocean carboxylic acids (Dominutti et al., 2022).

In contrast, the C_xH_y (aliphatics) ion family (m/z 13.00, m/z 15.02, m/z 16.03, etc.) contributes only 13.7 % to the MO-OOA total mass spectra intensity. Nitrogen-containing ion fragments constituted a very low portion of the signal (0.8 %), similarly to previous remote-ocean measurements (Ovadnevaite et al., 2011). The weak contribution from $C_2H_3O^+$ (3.16 %), which has been reported to be predominantly due to non-acid oxygenates (Ng et al., 2011a), suggests a considerable prevalence of ageing/oxidation during transport over the northeastern Atlantic Ocean. This is also further confirmed by the low m/z 43 : 44 ratio of 0.12 pointing to MO-OOA rather than less oxidized species (Ng et al., 2011). This factor of 0.78 and 1.17 for O : C ratio and H : C ratio, respectively, further agrees with MO-OOA reported at other similar locations (Fig. S4 in the Supplement). MO-OOA also has a strong contribution from CO_2^+ (25.7 %), which is assumed to originate mainly from acids or acid-derived compounds (Duplissy et al., 2011; Ng et al., 2011) that are known to be mostly water-soluble (Decesari et al., 2007) such as organic acids (e.g. meso-tartaric acid, meso-erythritol, tartaric acid, oxalic acid) formed from the oligomerization of small α-dicarbonyls (e.g. glyoxal) (Cui et al., 2022).

MO-OOA formation through ozonolysis is postulated based on a robust hourly averaged correlation ($R = 0.67$) of MO-OOA to O_3 across the entire observational period (Fig. S6b in the Supplement). Using the test of effective transfer entropy (Behrendt et al., 2019) further reveals the non-linear dynamics between O_3 and MO-OOA, indicating O_3 is a significant reactant in the formation of MO-OOA from its precursors with a transfer entropy value (Fig. 3) of 0.0144 and a value of effective transfer entropy of 0.0127 ± 0.0009 (p value < 0.05). In other words, there is a significant directional information flow between the two time series. Figure 3 also shows that MO-OOA is a mix of local (peat-OA) and regional marine influence (PMOA but also MSA-OA to a lesser extent), all eventually amounting to MO-OOA formation, with ozone contributing 3 times more information to MO-OOA than irradiance does. Although irradiance and ozone were measured on site and may not be as directly related to conditions of aerosol during transport, this finding aligns with studies showing O_3 to be a strong oxidation driver during summertime in the marine environment (Ovadnevaite et al., 2011), where unsaturated aliphatic chains (C=C double bonds) react with ozone to form oxidized compounds (Decesari et al., 2011).

3.2.2 Methanesulfonic acid organic aerosol (MSA-OA)

The mass profile of MSA-OA reveals that two oxygenated carbon families of CHO (sum of $C_xH_yO_k$ and $C_xH_yO_w$, where $k = 1$ and $w > 1$) dominate 53.4 % of the total mass spectra fraction, followed by aliphatics (pure hydrocarbon-like, $C_xH_y^+$), whose fraction accounts for 33.3 % (Fig. S5). MSA-OA is clearly identified owing to its substantial contribution from the $C_xS_y^+$ family (6 %) over other sources; this is in line with the $C_xS_y^+$ contribution (7 %) for MSA-OA also reported by Huang et al. (2018). The excellent corre-

lation ($R = 0.82$) between this factor and the $C_xS_y^+$ family (Fig. S6d) also further highlights the organosulfur nature of MSA-OA as opposed to other factors.

Similarly to results reported by Schmale et al. (2013), the correlation coefficient with the AMS database of the MSA-OA laboratory reference spectrum (Fig. S6a) is rather moderate ($R = 0.55$), although this factor spectra still allows for the precise identification of characteristic MSA ions at m/z 44.98 (CHS^+), m/z 47.00 (CH_3S^+), m/z 64.97 (HSO_2^+), m/z 77.98 ($CH_2SO_2^+$), m/z 77.99 ($CH_3SO_2^+$), and m/z 95.99 ($CH_4SO_3^+$). MSA-OA O : C and H : C ratios were 0.66 and 1.39, respectively, close to values (O : C of 0.54, H : C of 1.42) reported by Loh et al. (2023).

The MSA-OA C_xH_y family also features a typical CH_3^+ ion at m/z 15.02 that is absent from other factors. Similarly, the $C_xH_yO_w$ ($w = 1$) family features the tracers ions CH_2O^+ (8.2 %) and CH_3O^+ (2.4 %) which are heat-stress-related markers (Faiola et al., 2015) attributed to methyl jasmonate (MeJA) and possibly acrylic acid (Van Alstyne and Houser, 2003) or other oxylipin stress enzymes (Aguilera et al., 2022; Koteska et al., 2022) which are known to be emitted by kelp (Saha and Fink, 2022) or phytoplankton species (Koteska et al., 2022).

The $C_xS_y^+$ fragment family was dominated by CHS^+ (25.9 %), $CH_3SO_2^+$ (20.2 %), CH_2S^+ (12.2 %), $CH_4SO_3^+$ (7.5 %), CH_3SO^+ (7.2 %), $CH_2SO_2^+$ (6.9 %), $CH_4SO_2^+$ (5.45), CH_3S^+ (6.41 %), $C_2H_4SO_2$ (5.4 %), and CH_2SO^+ (2.5 %), which are common MSA ions found in the literature (Moschos et al., 2022). Overall, the $C_xH_y^+$ and $C_xS_y^+$ fragment ion families indicate a clear MSA fragmentation pattern with a characteristic high CH_3^+ relative intensity (13 %) typical of marine SOA in line with recent findings (Huang et al., 2018; Moschos et al., 2022).

Finally, MSA-OA correlated moderately (Fig. S6b) with particulate sulfate ($R = 0.51$), which is expected since dimethyl sulfide, released by phytoplankton, can be oxidized to either form MSA or sulfur dioxide and then to sulfuric acid, leading to their partitioning into the particulate phase (Mungall et al., 2018). Although MSA is often found in clusters with amine, dimethylamine, or trimethylamine (Bork et al., 2014; Chen et al., 2016; Paglione et al., 2024), the MSA spectrum minor methylamine contributions such as m/z 30 (CH_4N^+), m/z 41 ($C_3H_5^+$), and m/z 42 ($C_2H_4N^+$) (Malloy et al., 2009) were too sparse to assume involvement.

3.2.3 Primary marine organic aerosol (PMOA)

The high-resolution mass spectrum of this factor reveals that two CHO oxygenated carbon families (sum of $C_xH_yO_k$ and $C_xH_yO_w$, where $x = 1$ and $w > 1$) dominate 61.5 % of the total mass spectra, followed by aliphatics (pure hydrocarbon-like, C_xH_y), whose fraction accounts for 36.2 % of the total mass spectra signal (Fig. S5), aligning with previous findings reported by Ovadnevaite et al. (2011). The $C_xH_yO_w$ ($w = 1$) family features ion series (m/z 55.02, m/z 69.03, m/z 83.05, etc.) related to alkenyl groups, diunsaturates, cyclic alcohols, and ethers. Such a repartition of functional groups is consistent with previous reports of water-insoluble organics being formed in sea spray (O'Dowd et al., 2004; Ovadnevaite et al., 2011). Additionally, this factor mass spectrum closely resembles ($R = 0.99$) marine organic aerosol (MOA) mass spectra (Ovadnevaite et al., 2011) (Fig. S6a), and its O : C ratio of 0.66 and an H : C ratio of 1.16, respectively, are close to literature O : C values for sea spray (Ovadnevaite et al., 2011; Flerus et al., 2012; Willoughby et al., 2016) (Fig. S4).

The PMOA C_xH_y mass spectra family is dominated by the C_xH_{2y-3} ion series (m/z 39.02, m/z 53.03, m/z 67.05, etc.), indicating dienes, alkynes, and cycloalkene contributions, which are further confirmed by the presence of the C_xH_{2y-1} ion series (m/z 27.02, m/z 41.04, m/z 55.05, etc.), while the C_xH_{2y+1} family (m/z 43.05, m/z 57.07, m/z 83.08, etc.; $y > 2$) indicative of anthropogenically influenced refined hydrocarbons is absent from this factor mass spectrum. The marine biogenic origin of this factor is also indicated by the absence of alkanes (C_xH_{y+2}; m/z 16.03, m/z 58.08, m/z 72.09) which are typical of continental air masses (Lewis et al., 2021) and by its lack of correlation with eBC ($R = 0.17$), thereby excluding contribution from fossil hydrocarbons to PMOA. The C_xH_y family is also marked by alkyls (C_xH_{2y+1}; m/z 15.02, m/z 29.03, m/z 37.00, etc.), which have been reported to be dominant in sea spray during phytoplankton blooms as a possible result of phosphate cycling (Cavalli, 2004; Meador et al., 2017).

Prior atmospheric measurements have shown that PMOA containing a large fraction of alkenes and oxygenated functional groups (i.e. alcohols, ethers, aldehydes, ketones) are dominated by insoluble organic colloids and aggregates (Facchini et al., 2008; Rinaldi et al., 2020) composed of microgels derived from phytoplankton extracellular metabolic extraction and the adsorption organic pool rather than exopolymers produced from bacteria, with abacterial microgel aerosol being quite common and possibly accounting for 50 %–90 % or phytoplankton-derived organics (Bigg and Leck, 2008; Bates et al., 2012; Liu et al., 2023). These bacterial exopolymers would follow the makeup of ordinary bacterial cell fragments, which comprise approximately 55 % of nitrogen-containing organics and 10 % of carbohydrates (Schmale et al., 2013). The latter are accounted for by summing up pure carbohydrates (i.e. glucose, saccharose, mannitol, and glycogen) identified by typical fragments (Schmale et al., 2013; Schneider et al., 2011) at m/z 56.03 ($C_3H_4O^+$), m/z 60.02 ($C_2H_4O^+$), m/z 61.03 ($C_2H_5O^+$), and m/z 85.03 ($C_4H_5O^+$), only accounting for about 1.3 % of the total PMOA aerosol mass. Similarly, contributions from other bacterial tracers, such as glycogen at m/z 55.01 (1.36 %), mannitol at m/z 56.02 (0.4 %), and polysaccharide species at m/z 97.02 ($C_5H_5O_2^+$) and m/z 125.02 ($C_6H_5O_3^+$) (Glicker et al., 2022), were also relatively poor (0.7 %). All of this paired with below-detection-limit amino acids thus implies that the PMOA organic pool was largely shaped by abacte-

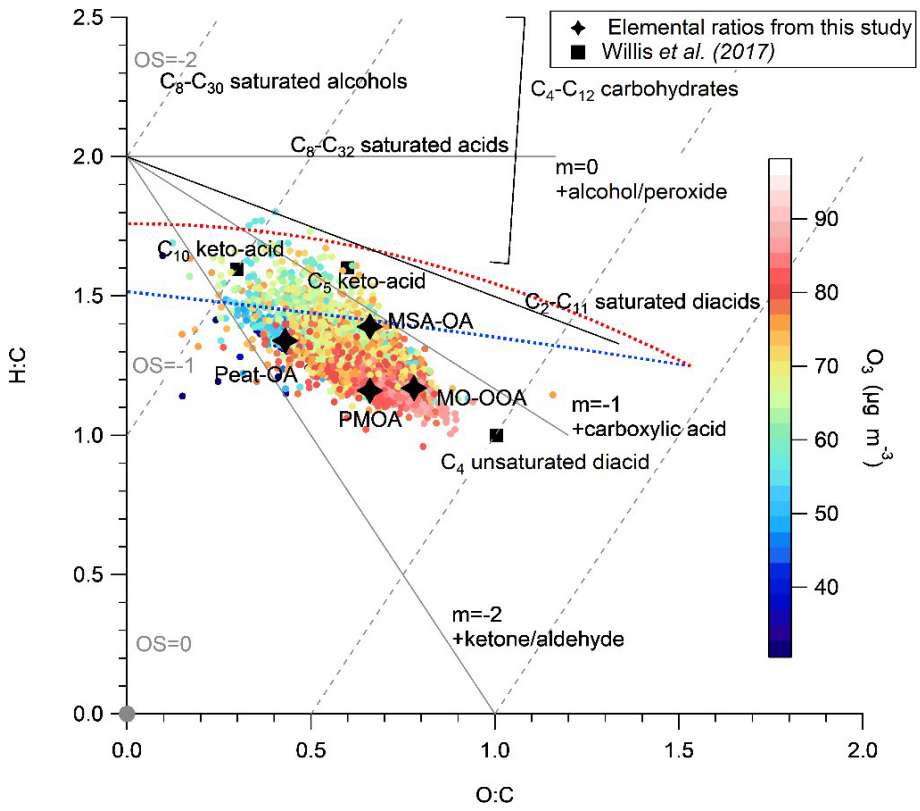

Figure 4. Relationship between the ToF-AMS-estimated hydrogen-to-carbon (H : C) and oxygen-to-carbon (O : C) ratios of organic species (Canagaratna et al., 2015) coloured by the O_3 mixing ratio; all observations above ToF-AMS detection limits are shown for the entire period. Grey lines represent the ambient range of O : C and H : C observed by Ng et al. (2011), while dashed lines represent the average carbon oxidation state (OSc ≈ 2× O : C–H : C) superimposed on the van Krevelen diagram (Ng et al., 2011; Kroll et al., 2011). Elemental composition of C_8–C_{30} saturated alcohols, C_8–C_{32} saturated acids, C_2–C_{11} saturated diacids, C_4 unsaturated diacid (maleic and fumaric acid), C_4–C_{12} carbohydrates (e.g. trehalose, erythritol, arabitol, mannitol, sucrose, galactose, glucose, and fructose), and C_5 and C_{10} keto-acids (levulinic and pinonic acid, respectively) are shown for reference (Willis et al., 2017).

rial processes. However, bacterial influence cannot be ruled out entirely as carbohydrates might have been processed by enzymes or acidity during air mass transport and subsequent ageing (Zeppenfeld et al., 2023). A potentially important tracer for this activity could be lactic acid, which has been observed before in sea spray owing to microorganisms fermenting sugars (Miyazaki et al., 2014; Paglione et al., 2024), although lactic acid itself still remains understudied in HR-ToF-AMS studies.

3.2.4 Peat-derived organic aerosol (peat-OA)

Although the measurement period is largely dominated by pristine ocean air masses, some residential heating influence is still observed owing to local peat burning. Peat-OA mass spectra are largely dominated by saturated alkanes and alkenes, amounting to 76.92 %, which is typical of peat. This factor mass spectrum correlates well ($R = 0.86$) with previous measurements of peat-OA in the city of Galway (Lin et al., 2017) (Fig. S6a). More specifically, the presence of aromatic ion series at m/z 77.03 ($C_6H_5^+$) and m/z 91.0.5 ($C_7H_7^+$) (Cubison et al., 2011) and the ratio between m/z 55.05 ($C_4H_7^+$) and m/z 57.07 ($C_4H_9^+$) of 1.74 as well as the ratio between m/z 43.05 ($C_3H_7^+$) and m/z 44.01 ($C_2H_3O^+$) of 1.03 all allow for the clear distinction of peat burning compared to other sources (Lin et al., 2017). Peat-OA was freshly emitted as evidenced by the pollution wind rose (Fig. S7e and f in the Supplement), and the concurrent increase along with eBC ($R = 0.72$) indicates that both were locally co-emitted within the PBL.

3.3 Elemental ratios – van Krevelen diagram

The van Krevelen (VK) diagram (Heald et al., 2010) provides valuable information on the chemical evolution of OA as demonstrated by subsequent marine aerosol studies (Ovadnevaite et al., 2014; Willis et al., 2017; Dada et al., 2022). The VK plot of the PMF factors identified in this study superimposed with bulk OA O : C and H : C values is depicted in Fig. 4. Overall, the bulk OA slope of −1.18 and $\overline{\text{OSc}}$ (carbon oxidation state) values spanning from −1.8 to 0.8 in the carbon oxidation state space indicate that higher levels of ox-

idation involving the generation of carboxylic acids and the subsequent breakdown of the carbon backbone are prevalent over the measurement period, which is consistent with MO-OOA functional groups (Heald et al.2010, Ng et al., 2011). The O : C ratios for MO-OOA, PMOA, and MSA-OA all fall within the range of 0.64–1.15 reported for diverse OOA factors from previous studies (Aiken et al., 2008; Jimenez et al., 2009). All PMF factors have H : C values lower than 2, which indicates that they all contain unsaturated carbons capable of reacting with O_3 (Ovadnevaite et al., 2011). This is evidenced by the flow analysis of effective transfer entropy (Behrendt et al., 2019) between peat-OA, PMOA, MO-OOA, MSA-OA, and O_3 values (Fig. 3), which indicates that peat-OA had the highest information transfer flow, making it the most susceptible to ozonolysis, closely followed by PMOA and, to a lesser extent, MSA-OA. Both peat-OA (O : C of 0.43, H : C of 1.34) and PMOA (O : C of 0.66, H : C of 1.16) VK positions broadly fall in the area consistent with lignin-like compounds (H : C of 0.6–1.5, O : C of 0.1–0.6; Park et al., 2022), which have been largely associated with terrestrial-origin OA (Jang et al., 2022) and found to be high in Arctic Ocean air masses as well (Choi et al., 2019), with authors reporting $\sim 30\,\%$ of the total assigned molecular formulae as marine lignin-like compounds. These lignin-like compounds are also known to oxidize and form humic-like molecules, characterized by polar carbonyl (keto and carboxyl) functional groups alongside hydrophobic aliphatic chains (Cavalli, 2004), broadly agreeing with MO-OOA functional groups.

MSA-OA (O : C of 0.66, H : C of 1.9) is then also examined by colouring the VK scatter plot (Fig. S8 in the Supplement) with the MSA-OA : SO_4 ratio, a proxy for biological marine source contributions from dimethyl sulfide (DMS; Chen et al., 2021), with values ranging from 0.001 (ubiquitous anthropogenic influences) to 0.354 (significant contribution from biological marine sources), with an average value of 0.102 in line with pristine conditions (Huang et al., 2018). Figure S8 shows that a high MSA-to-sulfate ratio was consistent with VK region for C_2–C_{12} saturated diacids and inconsistent with C_4–C_{12} carbohydrates and derivatives (trehalose, erythritol, arabitol, mannitol, sucrose, galactose, glucose, fructose, etc.), similarly to results reported for the summertime Arctic (Willis et al., 2017). However, as opposed to Arctic aerosol, with H : C ratios being higher, we report no association with VK areas for C_4 unsaturated diacids (e.g. maleic and fumaric acid) nor with C_{10} and C_5 keto-acids (levulinic and pinonic acid), which are aqueous photochemistry tracers from isoprene and α-pinene oxidation (Kołodziejczyk et al., 2019; Rapf et al., 2017). This is in line with the absence of other isoprene tracers, $C_4H_5^+$ (0.49 %) at m/z 53.03 and $C_5H_6O^+$ (0.18 %) at m/z 82.04 (Hu et al., 2015; Robinson et al., 2011), and monoterpenes tracers (Boyd et al., 2015), namely $C_5H_7^+$ at m/z 67.05 (0.15 %) and ($C_7H_7^+$) at 91.05 (0.15 %). This is also supported by the lack of covariance ($\mathrm{Cov}[X, Y] \approx 0$) between bulk CO_2^+, CO^+, and $C_2H_3O^+$ time series, also denoting non-acid carbonyl (naCO) absence (Yazdani et al., 2022), known to be derived from isoprene and monoterpenes (Russell et al., 2011). The reasons behind the absence of isoprene and monoterpene influence on OA in these findings are currently unclear, although processes such as surface ocean consumption or unexplored oxidations pathways could be a possibility (Benavent et al., 2022).

3.4 Air masses and source apportionment

The strongest MO-OOA (Fig. 5a) sources can be traced back northward along a cyclonic gradual crescent shape spreading from the Greenland Sea south of Cape Farewell (see Fig. S9 in the Supplement for ocean area toponomy). This culminates further with air mass origins spanning over the East Greenland Current (Denmark Strait), upwards to the Iceland Sea, south of Jan Mayen. MO-OOA is otherwise ubiquitous and shows contributions over the Newfoundland, Labrador, and Iceland basins as well as other areas. O_3 (Fig. 5b) shared an origin similar to MO-OOA, further confirming its role in MO-OOA formation. Overall, we observe aged polar air masses eventually flowing from Greenland to MHD. The sustained blockade and ageing of air masses over Greenland is known and attributed to summertime high-pressure systems surrounding this region, influenced by Arctic amplification (Pettersen et al., 2022; Preece et al., 2023), where the Irminger Current also acts as a hotspot for turbulent eddies and heat transport which might contribute to aerosol nucleation (Semper et al., 2022). Here the presence of a blocking anticyclone transition (Fig. S10 in the Supplement) leading to reduced cloud cover and warm-air advection might ultimately have contributed to an increase in aged SOA at the southern tip of Greenland, possibly owing to its orography.

The main MSA-OA (Fig. 5c) sources include the Iceland Basin and more specifically the Iceland–Faroe Ridge. This is consistent with literature highlighting the diversity of eukaryotic phytoplankton in the Icelandic marine environment, with the haptophyte coccolithophore *Emiliania huxleyi* being dominant during summertime (Cerfonteyn et al., 2023) owing to nutrient transport by acceleration of the North Atlantic Current (Oziel et al., 2020) and findings (O'Dowd et al., 2015; Mansour et al., 2023) indicating a concomitant MSA concentration uptick during summertime. MSA-OA also spans along the East Greenland Current (Denmark Strait), where wind-driven coastal upwelling (Håvik and Våge, 2018) might result in increased DMS emissions (Edtbauer et al., 2020). Likewise, MSA-OA extends moderately over diverse regions such as the northwestern European Basin, the Newfoundland Basin (where intense DMS fluxes have been reported; Bell et al., 2021), and the Labrador Sea.

PMOA (Fig. 5d) on the other hand strongly extends over the south of the Celtic Sea and west of the Bay of Biscay as well as western European Basin waters and are otherwise diffused all over the North Atlantic, with moderate intensity

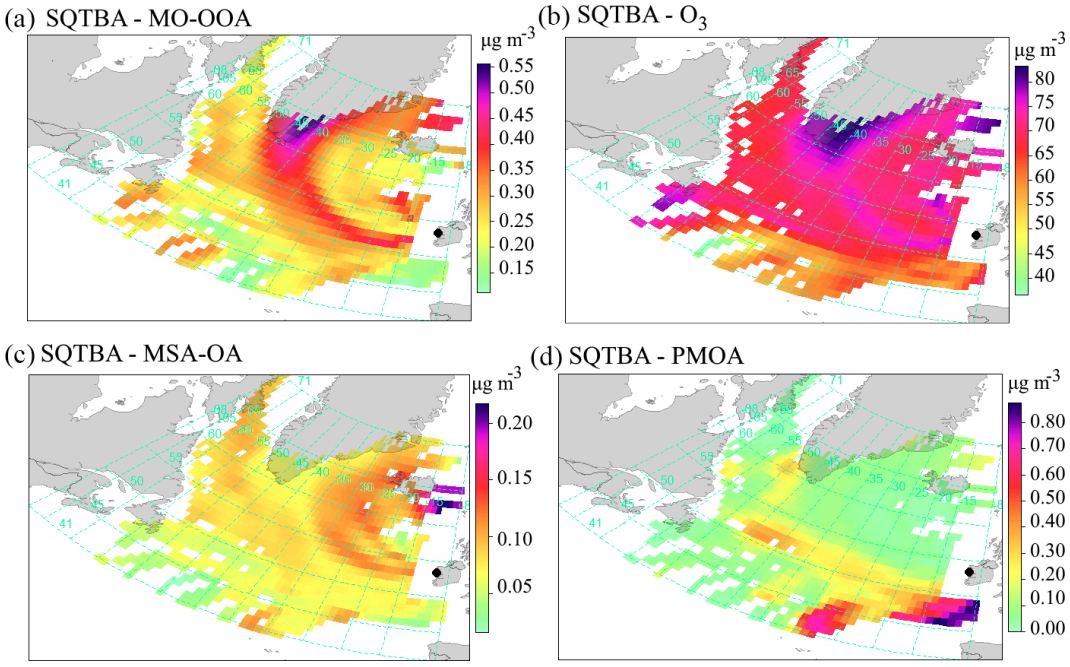

Figure 5. Simplified quantitative transport bias analysis (SQTBA). Gaussian air mass dispersion for PMF sources (PMOA, MO-OOA, MSA-OA) and O_3.

hotspots over the Newfoundland Basin (Davis Strait) possibly owing to an inflated subpolar gyre (Hátún et al., 2016).

Examination of NOBM model data (Fig. 6) further reveals distinct MSA-OA and PMOA patterns. MSA-OA overlaps with coccolithophore-dominated ecoregions as well as diatom ones. Similarly, diatoms also seem to contribute to PMOA sources, which is in line with recent results hypothesizing that diatoms have a greater atmospheric significance than other eukaryotes due to their observed enrichment in PMOA (Alsante et al., 2021), whereas association with coccolithophores appears much weaker than for MSA-OA. Another distinction lies in PMOA overlapping with chlorophytes (flagellates, *Phaeocystis* spp.) over the western European Basin. This geographic area hosts more than 512 chlorophyte species (Narayanaswamy et al., 2010), with recent reports of chlorophytes being one of the key contributors to marine productivity (Landwehr et al., 2021); further research is warranted to fully understand their role along with other phytoplankton in this region during summertime. Likewise, cyanobacteria (combination of *Synechococcus*, *Prochlorococcus*, and nitrogen fixers such as *Trichodesmium*) might also contribute to PMOA more sparsely, especially at lower latitudes in the North Atlantic as previously reported (Baer et al., 2017).

Here, calculated lagged correlations (Fig. 6) further pointed to MSA-OA being directly associated with coccolithophores (with a lag of −1 d) as well as diatoms (lag of −9 d); however no significant correlations were observed for either cyanobacteria or chlorophytes. As opposed to MSA-OA, the association between coccolithophores and PMOA does not appear as meaningful (their autocorrelations are not statistically significant). PMOA on the other hand is also associated with diatoms (lag of −5 d) and shows unique associations with chlorophytes (lag of −10 d) as well as cyanobacteria (lag of −11 d).

Overall, the association between OA-enriched sea spray time series and phytoplankton groups remains controversial owing to a wide range of governing mechanisms, as highlighted by previous studies using chlorophyll *a* as a proxy to calculate cross-correlation time lags over the North Atlantic which were found to vary between 8 (Rinaldi et al., 2013) and 24 d (O'Dowd et al., 2015) depending on the period and length of measurements.

Late-summer measurements (Mansour et al., 2020) show partially comparable lags to this study with a reported oceanic biological activity affecting aerosol properties within the order of 10–20 d. This delay roughly spans over the full phase transitions of the blooming to decaying of an algal bloom (Lehahn et al., 2014) and is linked to the release of organic matter transferable by sea spray aerosol (SSA) in surface seawater by the interaction with marine viruses causing the demise of phytoplankton blooms (O'Dowd et al., 2015).

Here, by focusing on the lagged correlations between PMF factors and specific phytoplankton groups rather than bulk OA and chlorophyll *a*, this study's findings indicate that PMOA is formed on a timescale of blooming to decay from cyanobacteria and chlorophytes (lags of −11 and −10 d, respectively) owing to atmospheric transport from the western

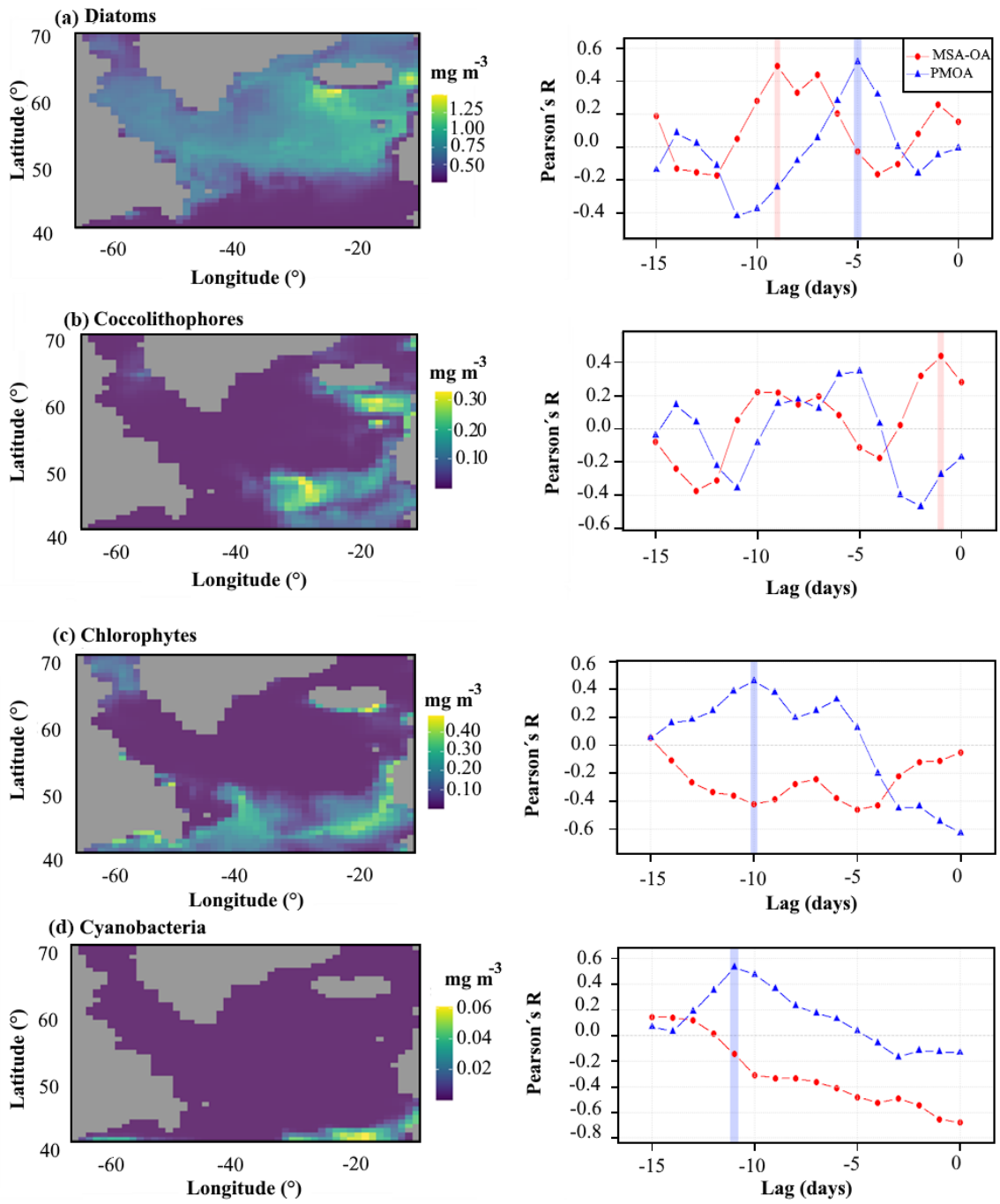

Figure 6. Time-averaged maps (0.67° × 1.25°) in August 2015 over the region of 37–82° N and 59° W–34° E of dominant phytoplankton groups from NOBM data (Gregg and Rousseaux, 2017; Buchard et al., 2017) and corresponding lagged cross-correlations for MSA-OA (red) and PMOA (blue) against **(a)** diatoms, **(b)** coccolithophores, **(c)** chlorophytes, and **(d)** cyanobacteria. The blue- and red-shaded areas correspond to maximum significant cross-correlations extracted from the autocorrelation function (ACF) with 95 % criteria.

European Basin, whereas overwhelming diatom influence results in a much shorter lag of −5 d. Additionally, MSA-OA is rapidly produced from coccolithophore blooms in 1–2 d. This reflects stressed, senescent, grazed, or virus-infected phytoplankton releasing high quantities of dimethylsulfoniopropionate (DMSP), which rapidly oxidizes to form MSA-OA (Mansour et al., 2020).

Finally, the interpretation of diatoms' influence on either MSA-OA or PMOA remains ambiguous. The −5 d lag with PMOA could hint at lipase activity with self-aggregation and formation of free fatty acids during the bloom phase, poten-

tially followed by a post-bloom phase (at a lag of −9 d with MSA-OA) with significantly different taxa. Alternatively, the −9 d lag with MSA-OA could have been caused by air advection from remote ecoregions near the Arctic that have been reported to host rich MSA-producing diatom communities not present in the southerly latitudes (Becagli et al., 2016).

4 Conclusions

This study leverages high-resolution online aerosol mass spectrometry source apportionment to investigate the chemical composition and sources of submicron organic aerosol representing the marine environment during a summertime period marked by phytoplankton blooms. The results emphasize balanced mass contributions from POA (PMOA and peat-OA) and SOA (MO-OOA and MSA-OA), with each category accounting for approximately 50 % of the total submicron organic aerosol mass, with distinct chemical compositions reflective of their varied origins.

One of this study's key findings is that summertime polar air masses undergo significant ozonolysis over the remote ocean, which happens to be largely driven by the ageing of Greenland blocked air masses and anticyclonic conditions. Transfer entropy is introduced here to explain the dynamics of ozonolysis in this context, revealing significant information transfer to MO-OOA during unsaturated-aliphatic-chain (C=C double bonds) breakdown of PMOA as well as MSA-OA to a lesser extent. However, this transfer entropy approach additionally shows that MO-OOA is also being formed locally from peat-OA oxidation; as such, further studies will aim at exactly delineating open-ocean vs. locally produced MO-OOA.

Another essential takeaway is that OA not only reflects atmospheric chemistry and meteorology but also may serve as an indicator of marine ecosystems (i.e. MSA-OA enzyme stress makers and PMOA phytoplankton extracellular metabolic process markers). Air mass trajectory analysis reveals the source aerosol–phytoplankton ecoregions. MSA-OA contributions are traced to the Iceland Basin and the Iceland–Faroe Ridge, with a rapid production burst (lag of 1–2 d) following coccolithophore blooms, whereas a relationship with diatoms shows a much longer lag (9 d), indicating fundamentally different oceanic biological processes. In contrast, PMOA is sourced from more diverse ecoregions (southern Celtic Sea, western European Basin, and Newfoundland Basin), with additional chlorophytes and cyanobacteria influences from more southerly latitudes. All of this suggests that different contributions of phytoplankton taxa to OA lead to specific m/z tracers and functional-group repartition (i.e. sulfides as coccolithophores tracers, aliphatics as tracers for diatoms), though further investigation is needed to explore the biological processes and ecoregion specificities influencing this relationship. Overall, this study demonstrates the complex aerosol chemistry and diverse geographic origins influencing POA and SOA formation in the northeastern Atlantic marine environment. Our findings emphasize the need for further long-term investigation to fully account for the various precursors and pathways contributing to OA, given their significant impacts on aerosol–climate interactions.

Data availability. Data are available upon request. The NASA Ocean Biogeochemical Model output data were obtained with the Giovanni online data system, developed and maintained by the NASA Goddard Earth Sciences Data and Information Services Center (GES DISC). The ERA5 boundary layer data are available at the Copernicus Climate Data Store portal (https://doi.org/10.24381/cds.adbb2d47; Hersbach et al., 2023, 2020).

Supplement. The supplement related to this article is available online at https://doi.org/10.5194/acp-25-4107-2025-supplement.

Author contributions. JO, CO'D, and DC designed the research. DC, JO, and KNF operated the instruments and verified the raw data. EC and JO produced the postprocessed data and figures. JO, CO'D, LL, DC, WX, and CL reedited the manuscript. EC wrote the paper with support from all authors, who commented on the paper.

Competing interests. The contact author has declared that none of the authors has any competing interests.

Disclaimer. Publisher's note: Copernicus Publications remains neutral with regard to jurisdictional claims made in the text, published maps, institutional affiliations, or any other geographical representation in this paper. While Copernicus Publications makes every effort to include appropriate place names, the final responsibility lies with the authors.

Acknowledgements. This work was supported by the Environmental Protection Agency (EPA) of Ireland; the Department of the Environment, Climate and Communications; and the University of Galway College of Science and Engineering Postgraduate Research Scholarship Scheme (grant no. 127407). Chunshui Lin acknowledges support from the International Partnership Program of the Chinese Academy of Sciences (grant no. 175GJHZ2022039FN). The authors would also like to acknowledge the support from the Science Foundation Ireland Frontiers for the Future Programme (SFI FFP; award no. 22/FFP-A/10611). Finally, we would also like to extend our gratitude to Seraphine Hauser for looking into geopotential height anomalies and producing Fig. S10.

Financial support. This research has been supported by the Science Foundation Ireland (SFI FFP award no. 22/FFP-A/10611) and the Institute of Urban Environment of the Chinese Academy of Sciences (grant no.175GJHZ2022039FN).

Review statement. This paper was edited by Eliza Harris and reviewed by two anonymous referees.

References

Aguilera, A., Distéfano, A., Jauzein, C., Correa-Aragunde, N., Martinez, D., Martin, M. V., and Sueldo, D. J.: Do photosynthetic cells communicate with each other during cell death? From cyanobacteria to vascular plants, J. Exp. Bot., 73, 7219–7242, https://doi.org/10.1093/jxb/erac363, 2022.

Aiken, A. C., DeCarlo, P. F., Kroll, J. H., Worsnop, D. R., Huffman, J. A., Docherty, K. S., Ulbrich, I. M., Mohr, C., Kimmel, J. R., Sueper, D., Sun, Y., Zhang, Q., Trimborn, A., Northway, M., Ziemann, P. J., Canagaratna, M. R., Onasch, T. B., Alfarra, M. R., Prevot, A. S. H., Dommen, J., Duplissy, J., Metzger, A., Baltensperger, U., and Jimenez, J. L.: O/C and OM/OC Ratios of Primary, Secondary, and Ambient Organic Aerosols with High-Resolution Time-of-Flight Aerosol Mass Spectrometry, Environ. Sci. Technol., 42, 4478–4485, https://doi.org/10.1021/es703009q, 2008.

Alsante, A. N., Thornton, D. C. O., and Brooks, S. D.: Ocean Aerobiology, Front. Microbiol., 12, 764178, https://doi.org/10.3389/fmicb.2021.764178, 2021.

Asch, R. G., Stock, C. A., and Sarmiento, J. L.: Climate change impacts on mismatches between phytoplankton blooms and fish spawning phenology, Glob. Change Biol., 25, 2544–2559, https://doi.org/10.1111/gcb.14650, 2019.

Baer, S. E., Lomas, M. W., Terpis, K. X., Mouginot, C., and Martiny, A. C.: Stoichiometry of *Prochlorococcus*, *Synechococcus*, and small eukaryotic populations in the western North Atlantic Ocean, Environ. Microbiol., 19, 1568–1583, https://doi.org/10.1111/1462-2920.13672, 2017.

Bahadur, R., Uplinger, T., Russell, L. M., Sive, B. C., Cliff, S. S., Millet, D. B., Goldstein, A., and Bates, T. S.: Phenol Groups in Northeastern U. S. Submicrometer Aerosol Particles Produced from Seawater Sources, Environ. Sci. Technol., 44, 2542–2548, https://doi.org/10.1021/es9032277, 2010.

Ban, Z., Hu, X., and Li, J.: Tipping points of marine phytoplankton to multiple environmental stressors, Nat. Clim. Change, 12, 1045–1051, https://doi.org/10.1038/s41558-022-01489-0, 2022.

Bates, T. S., Quinn, P. K., Frossard, A. A., Russell, L. M., Hakala, J., Petäjä, T., Kulmala, M., Covert, D. S., Cappa, C. D., Li, S.-M., Hayden, K. L., Nuaaman, I., McLaren, R., Massoli, P., Canagaratna, M. R., Onasch, T. B., Sueper, D., Worsnop, D. R., and Keene, W. C.: Measurements of ocean derived aerosol off the coast of California, J. Geophys. Res., 117, D00V15, https://doi.org/10.1029/2012JD017588, 2012.

Becagli, S., Lazzara, L., Marchese, C., Dayan, U., Ascanius, S. E., Cacciani, M., Caiazzo, L., Di Biagio, C., Di Iorio, T., Di Sarra, A., Eriksen, P., Fani, F., Giardi, F., Meloni, D., Muscari, G., Pace, G., Severi, M., Traversi, R., and Udisti, R.: Relationships linking primary production, sea ice melting, and biogenic aerosol in the Arctic, Atmos. Environ., 136, 1–15, https://doi.org/10.1016/j.atmosenv.2016.04.002, 2016.

Becagli, S., Amore, A., Caiazzo, L., Iorio, T. D., Sarra, A. D., Lazzara, L., Marchese, C., Meloni, D., Mori, G., Muscari, G., Nuccio, C., Pace, G., Severi, M., and Traversi, R.: Biogenic Aerosol in the Artic from Eight Years of MSA Data from Ny Ålesund (Svalbard Islands) and Thule (Greenland), Atmosphere, 10, 349, https://doi.org/10.3390/atmos10070349, 2019.

Bedford, J., Ostle, C., Johns, D. G., Atkinson, A., Best, M., Bresnan, E., Machairopoulou, M., Graves, C. A., Devlin, M., Milligan, A., Pitois, S., Mellor, A., Tett, P., and McQuatters-Gollop, A.: Lifeform indicators reveal large-scale shifts in plankton across the North-West European shelf, Glob. Change Biol., 26, 3482–3497, https://doi.org/10.1111/gcb.15066, 2020.

Behrendt, S., Dimpfl, T., Peter, F. J., and Zimmermann, D. J.: RTransferEntropy – Quantifying information flow between different time series using effective transfer entropy, SoftwareX, 10, 100265, https://doi.org/10.1016/j.softx.2019.100265, 2019.

Behrenfeld, M. J., Moore, R. H., Hostetler, C. A., Graff, J., Gaube, P., Russell, L. M., Chen, G., Doney, S. C., Giovannoni, S., Liu, H., Proctor, C., Bolaños, L. M., Baetge, N., Davie-Martin, C., Westberry, T. K., Bates, T. S., Bell, T. G., Bidle, K. D., Boss, E. S., Brooks, S. D., Cairns, B., Carlson, C., Halsey, K., Harvey, E. L., Hu, C., Karp-Boss, L., Kleb, M., Menden-Deuer, S., Morison, F., Quinn, P. K., Scarino, A. J., Anderson, B., Chowdhary, J., Crosbie, E., Ferrare, R., Hair, J. W., Hu, Y., Janz, S., Redemann, J., Saltzman, E., Shook, M., Siegel, D. A., Wisthaler, A., Martin, M. Y., and Ziemba, L.: The North Atlantic Aerosol and Marine Ecosystem Study (NAAMES): Science Motive and Mission Overview, Front. Mar. Sci., 6, 122, https://doi.org/10.3389/fmars.2019.00122, 2019.

Bell, T. G., Porter, J. G., Wang, W.-L., Lawler, M. J., Boss, E., Behrenfeld, M. J., and Saltzman, E. S.: Predictability of Seawater DMS During the North Atlantic Aerosol and Marine Ecosystem Study (NAAMES), Front. Mar. Sci., 7, 596763, https://doi.org/10.3389/fmars.2020.596763, 2021.

Benavent, N., Mahajan, A. S., Li, Q., Cuevas, C. A., Schmale, J., Angot, H., Jokinen, T., Quéléver, L. L. J., Blechschmidt, A.-M., Zilker, B., Richter, A., Serna, J. A., Garcia-Nieto, D., Fernandez, R. P., Skov, H., Dumitrascu, A., Simões Pereira, P., Abrahamsson, K., Bucci, S., Duetsch, M., Stohl, A., Beck, I., Laurila, T., Blomquist, B., Howard, D., Archer, S. D., Bariteau, L., Helmig, D., Hueber, J., Jacobi, H.-W., Posman, K., Dada, L., Daellenbach, K. R., and Saiz-Lopez, A.: Substantial contribution of iodine to Arctic ozone destruction, Nat. Geosci., 15, 770–773, https://doi.org/10.1038/s41561-022-01018-w, 2022.

Bian, H., Froyd, K., Murphy, D. M., Dibb, J., Darmenov, A., Chin, M., Colarco, P. R., da Silva, A., Kucsera, T. L., Schill, G., Yu, H., Bui, P., Dollner, M., Weinzierl, B., and Smirnov, A.: Observationally constrained analysis of sea salt aerosol in the marine atmosphere, Atmos. Chem. Phys., 19, 10773–10785, https://doi.org/10.5194/acp-19-10773-2019, 2019.

Bigg, E. K. and Leck, C.: The composition of fragments of bubbles bursting at the ocean surface, J. Geophys. Res., 113, D11209, https://doi.org/10.1029/2007JD009078, 2008.

Bork, N., Elm, J., Olenius, T., and Vehkamäki, H.: Methane sulfonic acid-enhanced formation of molecular clusters of sulfuric acid and dimethyl amine, Atmos. Chem. Phys., 14, 12023–12030, https://doi.org/10.5194/acp-14-12023-2014, 2014.

Boyd, C. M., Sanchez, J., Xu, L., Eugene, A. J., Nah, T., Tuet, W. Y., Guzman, M. I., and Ng, N. L.: Secondary organic aerosol formation from the β-pinene + NO_3 system: effect of humidity and peroxy radical fate, Atmos. Chem. Phys., 15, 7497–7522, https://doi.org/10.5194/acp-15-7497-2015, 2015.

Brüggemann, M., Hayeck, N., and George, C.: Interfacial photochemistry at the ocean surface is a global source of organic vapors and aerosols, Nat. Commun., 9, 2101, https://doi.org/10.1038/s41467-018-04528-7, 2018.

Buchard, V., Randles, C. A., Da Silva, A. M., Darmenov, A., Colarco, P. R., Govindaraju, R., Ferrare, R., Hair, J., Beyersdorf, A. J., Ziemba, L. D., and Yu, H.: The MERRA-2 Aerosol Reanalysis, 1980 Onward. Part II: Evaluation and Case Studies, J. Climate, 30, 6851–6872, https://doi.org/10.1175/JCLI-D-16-0613.1, 2017.

Canagaratna, M. R., Jayne, J. T., Jimenez, J. L., Allan, J. D., Alfarra, M. R., Zhang, Q., Onasch, T. B., Drewnick, F., Coe, H., Middlebrook, A., Delia, A., Williams, L. R., Trimborn, A. M., Northway, M. J., DeCarlo, P. F., Kolb, C. E., Davidovits, P., and Worsnop, D. R.: Chemical and microphysical characterization of ambient aerosols with the aerodyne aerosol mass spectrometer, Mass Spectrom. Rev., 26, 185–222, https://doi.org/10.1002/mas.20115, 2007.

Canagaratna, M. R., Jimenez, J. L., Kroll, J. H., Chen, Q., Kessler, S. H., Massoli, P., Hildebrandt Ruiz, L., Fortner, E., Williams, L. R., Wilson, K. R., Surratt, J. D., Donahue, N. M., Jayne, J. T., and Worsnop, D. R.: Elemental ratio measurements of organic compounds using aerosol mass spectrometry: characterization, improved calibration, and implications, Atmos. Chem. Phys., 15, 253–272, https://doi.org/10.5194/acp-15-253-2015, 2015.

Canonaco, F., Crippa, M., Slowik, J. G., Baltensperger, U., and Prévôt, A. S. H.: SoFi, an IGOR-based interface for the efficient use of the generalized multilinear engine (ME-2) for the source apportionment: ME-2 application to aerosol mass spectrometer data, Atmos. Meas. Tech., 6, 3649–3661, https://doi.org/10.5194/amt-6-3649-2013, 2013.

Canonaco, F., Tobler, A., Chen, G., Sosedova, Y., Slowik, J. G., Bozzetti, C., Daellenbach, K. R., El Haddad, I., Crippa, M., Huang, R.-J., Furger, M., Baltensperger, U., and Prévôt, A. S. H.: A new method for long-term source apportionment with time-dependent factor profiles and uncertainty assessment using SoFi Pro: application to 1 year of organic aerosol data, Atmos. Meas. Tech., 14, 923–943, https://doi.org/10.5194/amt-14-923-2021, 2021.

Carslaw, K. S., Gordon, H., Hamilton, D. S., Johnson, J. S., Regayre, L. A., Yoshioka, M., and Pringle, K. J.: Aerosols in the Pre-industrial Atmosphere, Curr. Clim. Change Rep., 3, 1–15, https://doi.org/10.1007/s40641-017-0061-2, 2017.

Cavalli, F.: Advances in characterization of size-resolved organic matter in marine aerosol over the North Atlantic, J. Geophys. Res., 109, D24215, https://doi.org/10.1029/2004JD005137, 2004.

Ceburnis, D., Garbaras, A., Szidat, S., Rinaldi, M., Fahrni, S., Perron, N., Wacker, L., Leinert, S., Remeikis, V., Facchini, M. C., Prevot, A. S. H., Jennings, S. G., Ramonet, M., and O'Dowd, C. D.: Quantification of the carbonaceous matter origin in submicron marine aerosol by ^{13}C and ^{14}C isotope analysis, Atmos. Chem. Phys., 11, 8593–8606, https://doi.org/10.5194/acp-11-8593-2011, 2011.

Cerfonteyn, M., Groben, R., Vaulot, D., Guðmundsson, K., Vannier, P., Pérez-Hernández, M. D., and Marteinsson, V. Þ.: The distribution and diversity of eukaryotic phytoplankton in the Icelandic marine environment, Sci. Rep., 13, 8519, https://doi.org/10.1038/s41598-023-35537-2, 2023.

Chen, D., Shen, Y., Wang, J., Gao, Y., Gao, H., and Yao, X.: Mapping gaseous dimethylamine, trimethylamine, ammonia, and their particulate counterparts in marine atmospheres of China's marginal seas – Part 1: Differentiating marine emission from continental transport, Atmos. Chem. Phys., 21, 16413–16425, https://doi.org/10.5194/acp-21-16413-2021, 2021.

Chen, H., Varner, M. E., Gerber, R. B., and Finlayson-Pitts, B. J.: Reactions of Methanesulfonic Acid with Amines and Ammonia as a Source of New Particles in Air, J. Phys. Chem. B, 120, 1526–1536, https://doi.org/10.1021/acs.jpcb.5b07433, 2016.

Choi, J. H., Jang, E., Yoon, Y. J., Park, J. Y., Kim, T.-W., Becagli, S., Caiazzo, L., Cappelletti, D., Krejci, R., Eleftheriadis, K., Park, K.-T., and Jang, K. S.: Influence of Biogenic Organics on the Chemical Composition of Arctic Aerosols, Global Biogeochem. Cy., 33, 1238–1250, https://doi.org/10.1029/2019GB006226, 2019.

Cochran, R. E., Laskina, O., Trueblood, J. V., Estillore, A. D., Morris, H. S., Jayarathne, T., Sultana, C. M., Lee, C., Lin, P., Laskin, J., Laskin, A., Dowling, J. A., Qin, Z., Cappa, C. D., Bertram, T. H., Tivanski, A. V., Stone, E. A., Prather, K. A., and Grassian, V. H.: Molecular Diversity of Sea Spray Aerosol Particles: Impact of Ocean Biology on Particle Composition and Hygroscopicity, Chem, 2, 655–667, https://doi.org/10.1016/j.chempr.2017.03.007, 2017.

Crippa, M., El Haddad, I., Slowik, J. G., DeCarlo, P. F., Mohr, C., Heringa, M. F., Chirico, R., Marchand, N., Sciare, J., Baltensperger, U., and Prévôt, A. S. H.: Identification of marine and continental aerosol sources in Paris using high resolution aerosol mass spectrometry, J. Geophys. Res.-Atmos., 118, 1950–1963, https://doi.org/10.1002/jgrd.50151, 2013.

Croft, B., Martin, R. V., Moore, R. H., Ziemba, L. D., Crosbie, E. C., Liu, H., Russell, L. M., Saliba, G., Wisthaler, A., Müller, M., Schiller, A., Galí, M., Chang, R. Y.-W., McDuffie, E. E., Bilsback, K. R., and Pierce, J. R.: Factors controlling marine aerosol size distributions and their climate effects over the northwest Atlantic Ocean region, Atmos. Chem. Phys., 21, 1889–1916, https://doi.org/10.5194/acp-21-1889-2021, 2021.

Cubison, M. J., Ortega, A. M., Hayes, P. L., Farmer, D. K., Day, D., Lechner, M. J., Brune, W. H., Apel, E., Diskin, G. S., Fisher, J. A., Fuelberg, H. E., Hecobian, A., Knapp, D. J., Mikoviny, T., Riemer, D., Sachse, G. W., Sessions, W., Weber, R. J., Weinheimer, A. J., Wisthaler, A., and Jimenez, J. L.: Effects of aging on organic aerosol from open biomass burning smoke in aircraft and laboratory studies, Atmos. Chem. Phys., 11, 12049–12064, https://doi.org/10.5194/acp-11-12049-2011, 2011.

Cui, S., Huang, D. D., Wu, Y., Wang, J., Shen, F., Xian, J., Zhang, Y., Wang, H., Huang, C., Liao, H., and Ge, X.: Chemical properties, sources and size-resolved hygroscopicity of submicron black-carbon-containing aerosols in urban Shanghai, Atmos. Chem. Phys., 22, 8073–8096, https://doi.org/10.5194/acp-22-8073-2022, 2022.

Dada, L., Angot, H., Beck, I., Baccarini, A., Quéléver, L. L. J., Boyer, M., Laurila, T., Brasseur, Z., Jozef, G., De Boer, G., Shupe, M. D., Henning, S., Bucci, S., Dütsch, M., Stohl, A., Petäjä, T., Daellenbach, K. R., Jokinen, T., and Schmale, J.: A central arctic extreme aerosol event triggered by a warm air-mass intrusion, Nat. Commun., 13, 5290, https://doi.org/10.1038/s41467-022-32872-2, 2022.

DeCarlo, P. F., Kimmel, J. R., Trimborn, A., Northway, M. J., Jayne, J. T., Aiken, A. C., Gonin, M., Fuhrer, K., Horvath, T., Docherty, K. S., Worsnop, D. R., and Jimenez, J. L.: Field-Deployable, High-Resolution, Time-of-Flight Aerosol Mass Spectrometer, Anal. Chem., 78, 8281–8289, https://doi.org/10.1021/ac061249n, 2006.

Decesari, S., Mircea, M., Cavalli, F., Fuzzi, S., Moretti, F., Tagliavini, E., and Facchini, M. C.: Source Attribution of Water-Soluble Organic Aerosol by Nuclear Magnetic Resonance Spectroscopy, Environ. Sci. Technol., 41, 2479–2484, https://doi.org/10.1021/es061711l, 2007.

Decesari, S., Finessi, E., Rinaldi, M., Paglione, M., Fuzzi, S., Stephanou, E. G., Tziaras, T., Spyros, A., Ceburnis, D., O'Dowd, C., Dall'Osto, M., Harrison, R. M., Allan, J., Coe, H., and Facchini, M. C.: Primary and secondary marine organic aerosols over the North Atlantic Ocean during the MAP experiment, J. Geophys. Res.-Atmos., 116, https://doi.org/10.1029/2011JD016204, 2011.

Derwent, R. G., Simmonds, P. G., and Collins, W. J.: Ozone and carbon monoxide measurements at a remote maritime location, mace head, Ireland, from 1990 to 1992, Atmos. Environ., 28, 2623–2637, https://doi.org/10.1016/1352-2310(94)90436-7, 1994.

Derwent, R. G., Manning, A. J., Simmonds, P. G., Spain, T. G., and O'Doherty, S.: Long-term trends in ozone in baseline and European regionally-polluted air at Mace Head, Ireland over a 30-year period, Atmos. Environ., 179, 279–287, https://doi.org/10.1016/j.atmosenv.2018.02.024, 2018.

Dominutti, P. A., Chevassus, E., Baray, J.-L., Jaffrezo, J.-L., Borbon, A., Colomb, A., Deguillaume, L., El Gdachi, S., Houdier, S., Leriche, M., Metzger, J.-M., Rocco, M., Tulet, P., Sellegri, K., and Freney, E.: Evaluation of the Sources, Precursors, and Processing of Aerosols at a High-Altitude Tropical Site, ACS Earth Space Chem., 6, 2412–2431, https://doi.org/10.1021/acsearthspacechem.2c00149, 2022.

Drewnick, F., Hings, S. S., Alfarra, M. R., Prevot, A. S. H., and Borrmann, S.: Aerosol quantification with the Aerodyne Aerosol Mass Spectrometer: detection limits and ionizer background effects, Atmos. Meas. Tech., 2, 33–46, https://doi.org/10.5194/amt-2-33-2009, 2009.

Duplissy, J., DeCarlo, P. F., Dommen, J., Alfarra, M. R., Metzger, A., Barmpadimos, I., Prevot, A. S. H., Weingartner, E., Tritscher, T., Gysel, M., Aiken, A. C., Jimenez, J. L., Canagaratna, M. R., Worsnop, D. R., Collins, D. R., Tomlinson, J., and Baltensperger, U.: Relating hygroscopicity and composition of organic aerosol particulate matter, Atmos. Chem. Phys., 11, 1155–1165, https://doi.org/10.5194/acp-11-1155-2011, 2011.

Edtbauer, A., Stönner, C., Pfannerstill, E. Y., Berasategui, M., Walter, D., Crowley, J. N., Lelieveld, J., and Williams, J.: A new marine biogenic emission: methane sulfonamide (MSAM), dimethyl sulfide (DMS), and dimethyl sulfone ($DMSO_2$) measured in air over the Arabian Sea, Atmos. Chem. Phys., 20, 6081–6094, https://doi.org/10.5194/acp-20-6081-2020, 2020.

Etminan, M., Myhre, G., Highwood, E. J., and Shine, K. P.: Radiative forcing of carbon dioxide, methane, and nitrous oxide: A significant revision of the methane radiative forcing, Geophys. Res. Lett., 43, 12614–12623, https://doi.org/10.1002/2016GL071930, 2016.

Facchini, M. C., Rinaldi, M., Decesari, S., Carbone, C., Finessi, E., Mircea, M., Fuzzi, S., Ceburnis, D., Flanagan, R., Nilsson, E. D., de Leeuw, G., Martino, M., Woeltjen, J., and O'Dowd, C. D.: Primary submicron marine aerosol dominated by insoluble organic colloids and aggregates, Geophys. Res. Lett., 35, L17814, https://doi.org/10.1029/2008GL034210, 2008.

Faiola, C. L., Wen, M., and VanReken, T. M.: Chemical characterization of biogenic secondary organic aerosol generated from plant emissions under baseline and stressed conditions: inter- and intra-species variability for six coniferous species, Atmos. Chem. Phys., 15, 3629–3646, https://doi.org/10.5194/acp-15-3629-2015, 2015.

Flerus, R., Lechtenfeld, O. J., Koch, B. P., McCallister, S. L., Schmitt-Kopplin, P., Benner, R., Kaiser, K., and Kattner, G.: A molecular perspective on the ageing of marine dissolved organic matter, Biogeosciences, 9, 1935–1955, https://doi.org/10.5194/bg-9-1935-2012, 2012.

Florou, K., Liangou, A., Kaltsonoudis, C., Louvaris, E., Tasoglou, A., Patoulias, D., Kouvarakis, G., Kalivitis, N., Kourtchev, I., Kalberer, M., Tsagkaraki, M., Mihalopoulos, N., and Pandis, S. N.: Chemical characterization and sources of background aerosols in the eastern Mediterranean, Atmos. Environ., 324, 120423, https://doi.org/10.1016/j.atmosenv.2024.120423, 2024.

Fossum, K. N., Ovadnevaite, J., Ceburnis, D., Dall'Osto, M., Marullo, S., Bellacicco, M., Simó, R., Liu, D., Flynn, M., Zuend, A., and O'Dowd, C.: Summertime Primary and Secondary Contributions to Southern Ocean Cloud Condensation Nuclei, Sci. Rep., 8, 13844, https://doi.org/10.1038/s41598-018-32047-4, 2018.

Fröhlich, R., Crenn, V., Setyan, A., Belis, C. A., Canonaco, F., Favez, O., Riffault, V., Slowik, J. G., Aas, W., Aijälä, M., Alastuey, A., Artiñano, B., Bonnaire, N., Bozzetti, C., Bressi, M., Carbone, C., Coz, E., Croteau, P. L., Cubison, M. J., Esser-Gietl, J. K., Green, D. C., Gros, V., Heikkinen, L., Herrmann, H., Jayne, J. T., Lunder, C. R., Minguillón, M. C., Močnik, G., O'Dowd, C. D., Ovadnevaite, J., Petralia, E., Poulain, L., Priestman, M., Ripoll, A., Sarda-Estève, R., Wiedensohler, A., Baltensperger, U., Sciare, J., and Prévôt, A. S. H.: ACTRIS ACSM intercomparison – Part 2: Intercomparison of ME-2 organic source apportionment results from 15 individual, co-located aerosol mass spectrometers, Atmos. Meas. Tech., 8, 2555–2576, https://doi.org/10.5194/amt-8-2555-2015, 2015.

Giordano, M. R., Kalnajs, L. E., Avery, A., Goetz, J. D., Davis, S. M., and DeCarlo, P. F.: A missing source of aerosols in Antarctica – beyond long-range transport, phytoplankton, and photochemistry, Atmos. Chem. Phys., 17, 1–20, https://doi.org/10.5194/acp-17-1-2017, 2017.

Glicker, H. S., Lawler, M. J., Chee, S., Resch, J., Garofalo, L. A., Mayer, K. J., Prather, K. A., Farmer, D. K., and Smith, J. N.: Chemical Composition of an Ultrafine Sea Spray Aerosol during the Sea Spray Chemistry and Particle Evolution Experiment, ACS Earth Space Chem., 6, 1914–1923, https://doi.org/10.1021/acsearthspacechem.2c00127, 2022.

Goldstein, A. H. and Galbally, I. E.: Known and Unexplored Organic Constituents in the Earth's Atmosphere, Environ. Sci. Technol., 41, 1514–1521, https://doi.org/10.1021/es072476p, 2007.

Gregg, W. and Rousseaux, C.: NASA Ocean Biogeochemical Model assimilating satellite chlorophyll data global daily

VR2017, Greenbelt, MD, USA, Goddard Earth Sciences Data and Information Services Center (GES DISC) [data set], https://doi.org/10.5067/PT6TXZKSHBW9 (last access: 14 December 2023), 2017.

Grigas, T., Ovadnevaite, J., Ceburnis, D., Moran, E., McGovern, F. M., Jennings, S. G., and O'Dowd, C.: Sophisticated Clean Air Strategies Required to Mitigate Against Particulate Organic Pollution, Sci. Rep., 7, 44737, https://doi.org/10.1038/srep44737, 2017.

Guo, J., Zhang, J., Yang, K., Liao, H., Zhang, S., Huang, K., Lv, Y., Shao, J., Yu, T., Tong, B., Li, J., Su, T., Yim, S. H. L., Stoffelen, A., Zhai, P., and Xu, X.: Investigation of near-global daytime boundary layer height using high-resolution radiosondes: first results and comparison with ERA5, MERRA-2, JRA-55, and NCEP-2 reanalyses, Atmos. Chem. Phys., 21, 17079–17097, https://doi.org/10.5194/acp-21-17079-2021, 2021.

Hallquist, M., Wenger, J. C., Baltensperger, U., Rudich, Y., Simpson, D., Claeys, M., Dommen, J., Donahue, N. M., George, C., Goldstein, A. H., Hamilton, J. F., Herrmann, H., Hoffmann, T., Iinuma, Y., Jang, M., Jenkin, M. E., Jimenez, J. L., Kiendler-Scharr, A., Maenhaut, W., McFiggans, G., Mentel, Th. F., Monod, A., Prévôt, A. S. H., Seinfeld, J. H., Surratt, J. D., Szmigielski, R., and Wildt, J.: The formation, properties and impact of secondary organic aerosol: current and emerging issues, Atmos. Chem. Phys., 9, 5155–5236, https://doi.org/10.5194/acp-9-5155-2009, 2009.

Hátún, H., Lohmann, K., Matei, D., Jungclaus, J. H., Pacariz, S., Bersch, M., Gislason, A., Ólafsson, J., and Reid, P. C.: An inflated subpolar gyre blows life toward the northeastern Atlantic, Prog. Oceanogr., 147, 49–66, https://doi.org/10.1016/j.pocean.2016.07.009, 2016.

Håvik, L. and Våge, K.: Wind-Driven Coastal Upwelling and Downwelling in the Shelfbreak East Greenland Current, J. Geophys. Res.-Oceans, 123, 6106–6115, https://doi.org/10.1029/2018JC014273, 2018.

Heald, C. L., Kroll, J. H., Jimenez, J. L., Docherty, K. S., DeCarlo, P. F., Aiken, A. C., Chen, Q., Martin, S. T., Farmer, D. K., and Artaxo, P.: A simplified description of the evolution of organic aerosol composition in the atmosphere, Geophys. Res. Lett., 37, L08803, https://doi.org/10.1029/2010GL042737, 2010.

Hersbach, H., Bell, B., Berrisford, P., Hirahara, S., Horányi, A., Muñoz-Sabater, J., Nicolas, J., Peubey, C., Radu, R., Schepers, D., Simmons, A., Soci, C., Abdalla, S., Abellan, X., Balsamo, G., Bechtold, P., Biavati, G., Bidlot, J., Bonavita, M., Chiara, G., Dahlgren, P., Dee, D., Diamantakis, M., Dragani, R., Flemming, J., Forbes, R., Fuentes, M., Geer, A., Haimberger, L., Healy, S., Hogan, R. J., Hólm, E., Janisková, M., Keeley, S., Laloyaux, P., Lopez, P., Lupu, C., Radnoti, G., Rosnay, P., Rozum, I., Vamborg, F., Villaume, S., and Thépaut, J.: The ERA5 global reanalysis, Q. J. Roy. Meteor. Soc., 146, 1999–2049, https://doi.org/10.1002/qj.3803, 2020.

Hersbach, H., Bell, B., Berrisford, P., Biavati, G., Horányi, A., Muñoz Sabater, J., Nicolas, J., Peubey, C., Radu, R., Rozum, I., Schepers, D., Simmons, A., Soci, C., Dee, D., and Thépaut, J.-N.: ERA5 hourly data on single levels from 1940 to present, Copernicus Climate Change Service (C3S) Climate Data Store (CDS) [data set], https://doi.org/10.24381/cds.adbb2d47 (last access: 14 December 2023), 2023.

Hodshire, A. L., Campuzano-Jost, P., Kodros, J. K., Croft, B., Nault, B. A., Schroder, J. C., Jimenez, J. L., and Pierce, J. R.: The potential role of methanesulfonic acid (MSA) in aerosol formation and growth and the associated radiative forcings, Atmos. Chem. Phys., 19, 3137–3160, https://doi.org/10.5194/acp-19-3137-2019, 2019.

Holland, M. M., Louchart, A., Artigas, L. F., Ostle, C., Atkinson, A., Rombouts, I., Graves, C. A., Devlin, M., Heyden, B., Machairopoulou, M., Bresnan, E., Schilder, J., Jakobsen, H. H., Lloyd-Hartley, H., Tett, P., Best, M., Goberville, E., and McQuatters-Gollop, A.: Major declines in NE Atlantic plankton contrast with more stable populations in the rapidly warming North Sea, Sci. Total Environ., 898, 165505, https://doi.org/10.1016/j.scitotenv.2023.165505, 2023.

Hu, W. W., Campuzano-Jost, P., Palm, B. B., Day, D. A., Ortega, A. M., Hayes, P. L., Krechmer, J. E., Chen, Q., Kuwata, M., Liu, Y. J., de Sá, S. S., McKinney, K., Martin, S. T., Hu, M., Budisulistiorini, S. H., Riva, M., Surratt, J. D., St. Clair, J. M., Isaacman-Van Wertz, G., Yee, L. D., Goldstein, A. H., Carbone, S., Brito, J., Artaxo, P., de Gouw, J. A., Koss, A., Wisthaler, A., Mikoviny, T., Karl, T., Kaser, L., Jud, W., Hansel, A., Docherty, K. S., Alexander, M. L., Robinson, N. H., Coe, H., Allan, J. D., Canagaratna, M. R., Paulot, F., and Jimenez, J. L.: Characterization of a real-time tracer for isoprene epoxydiols-derived secondary organic aerosol (IEPOX-SOA) from aerosol mass spectrometer measurements, Atmos. Chem. Phys., 15, 11807–11833, https://doi.org/10.5194/acp-15-11807-2015, 2015.

Huang, S., Wu, Z., Poulain, L., van Pinxteren, M., Merkel, M., Assmann, D., Herrmann, H., and Wiedensohler, A.: Source apportionment of the organic aerosol over the Atlantic Ocean from 53° N to 53° S: significant contributions from marine emissions and long-range transport, Atmos. Chem. Phys., 18, 18043–18062, https://doi.org/10.5194/acp-18-18043-2018, 2018.

Huffman, J. A., Jayne, J. T., Drewnick, F., Aiken, A. C., Onasch, T., Worsnop, D. R., and Jimenez, J. L.: Design, Modeling, Optimization, and Experimental Tests of a Particle Beam Width Probe for the Aerodyne Aerosol Mass Spectrometer, Aerosol Sci. Tech., 39, 1143–1163, https://doi.org/10.1080/02786820500423782, 2005.

Jang, J., Park, J., Park, J., Yoon, Y. J., Dall'Osto, M., Park, K.-T., Jang, E., Lee, J., Cho, K. H., and Lee, B. Y.: Ocean–atmosphere interactions: Different organic components across pacific and southern oceans, Sci. Total Environ., 878, 162969, https://doi.org/10.2139/ssrn.4290253, 2022.

Jennings, S. G., Kleefeld, C., O'Dowd, C. D., Junker, C., Spain, T. G., O'Brien, P., Roddy, A. F., and O'Connor, T. C.: Mace Head Atmospheric Research Station – characterization of aerosol radiative parameters, Boreal Environ. Res., 8, 303–314, 2003.

Jimenez, J. L., Canagaratna, M. R., Donahue, N. M., Prevot, A. S. H., Zhang, Q., Kroll, J. H., DeCarlo, P. F., Allan, J. D., Coe, H., Ng, N. L., Aiken, A. C., Docherty, K. S., Ulbrich, I. M., Grieshop, A. P., Robinson, A. L., Duplissy, J., Smith, J. D., Wilson, K. R., Lanz, V. A., Hueglin, C., Sun, Y. L., Tian, J., Laaksonen, A., Raatikainen, T., Rautiainen, J., Vaattovaara, P., Ehn, M., Kulmala, M., Tomlinson, J. M., Collins, D. R., Cubison, M. J., E., Dunlea, J., Huffman, J. A., Onasch, T. B., Alfarra, M. R., Williams, P. I., Bower, K., Kondo, Y., Schneider, J., Drewnick, F., Borrmann, S., Weimer, S., Demerjian, K., Salcedo, D., Cottrell, L., Griffin, R., Takami, A., Miyoshi, T., Hatakeyama, S.,

Shimono, A., Sun, J. Y., Zhang, Y. M., Dzepina, K., Kimmel, J. R., Sueper, D., Jayne, J. T., Herndon, S. C., Trimborn, A. M., Williams, L. R., Wood, E. C., Middlebrook, A. M., Kolb, C. E., Baltensperger, U., and Worsnop, D. R.: Evolution of Organic Aerosols in the Atmosphere, Science, 326, 1525–1529, https://doi.org/10.1126/science.1180353, 2009.

Kahnert, M. and Kanngießer, F.: Optical properties of marine aerosol: modelling the transition from dry, irregularly shaped crystals to brine-coated, dissolving salt particles, J. Quant. Spectrosc. Ra., 295, 108408, https://doi.org/10.1016/j.jqsrt.2022.108408, 2023.

Karl, M., Leck, C., Coz, E., and Heintzenberg, J.: Marine nanogels as a source of atmospheric nanoparticles in the high Arctic, Geophys. Res. Lett., 40, 3738–3743, https://doi.org/10.1002/grl.50661, 2013.

Kawamura, K. and Bikkina, S.: A review of dicarboxylic acids and related compounds in atmospheric aerosols: Molecular distributions, sources and transformation, Atmos. Res., 170, 140–160, https://doi.org/10.1016/j.atmosres.2015.11.018, 2016.

Kirkby, J., Duplissy, J., Sengupta, K., Frege, C., Gordon, H., Williamson, C., Heinritzi, M., Simon, M., Yan, C., Almeida, J., Tröstl, J., Nieminen, T., Ortega, I. K., Wagner, R., Adamov, A., Amorim, A., Bernhammer, A.-K., Bianchi, F., Breitenlechner, M., Brilke, S., Chen, X., Craven, J., Dias, A., Ehrhart, S., Flagan, R. C., Franchin, A., Fuchs, C., Guida, R., Hakala, J., Hoyle, C. R., Jokinen, T., Junninen, H., Kangasluoma, J., Kim, J., Krapf, M., Kürten, A., Laaksonen, A., Lehtipalo, K., Makhmutov, V., Mathot, S., Molteni, U., Onnela, A., Peräkylä, O., Piel, F., Petäjä, T., Praplan, A. P., Pringle, K., Rap, A., Richards, N. A. D., Riipinen, I., Rissanen, M. P., Rondo, L., Sarnela, N., Schobesberger, S., Scott, C. E., Seinfeld, J. H., Sipilä, M., Steiner, G., Stozhkov, Y., Stratmann, F., Tomé, A., Virtanen, A., Vogel, A. L., Wagner, A. C., Wagner, P. E., Weingartner, E., Wimmer, D., Winkler, P. M., Ye, P., Zhang, X., Hansel, A., Dommen, J., Donahue, N. M., Worsnop, D. R., Baltensperger, U., Kulmala, M., Carslaw, K. S., and Curtius, J.: Ion-induced nucleation of pure biogenic particles, Nature, 533, 521–526, https://doi.org/10.1038/nature17953, 2016.

Kołodziejczyk, A., Pyrcz, P., Pobudkowska, A., Błaziak, K., and Szmigielski, R.: Physicochemical Properties of Pinic, Pinonic, Norpinic, and Norpinonic Acids as Relevant α-Pinene Oxidation Products, J. Phys. Chem. B, 123, 8261–8267, https://doi.org/10.1021/acs.jpcb.9b05211, 2019.

Koteska, D., Sanchez Garcia, S., Wagner-Döbler, I., and Schulz, S.: Identification of Volatiles of the Dinoflagellate Prorocentrum cordatum, Mar. Drugs, 20, 371, https://doi.org/10.3390/md20060371, 2022.

Kroll, J. A., Frandsen, B. N., Kjaergaard, H. G., and Vaida, V.: Atmospheric Hydroxyl Radical Source: Reaction of Triplet SO_2 and Water, J. Phys. Chem. A, 122, 4465–4469, https://doi.org/10.1021/acs.jpca.8b03524, 2018.

Kroll, J. H., Donahue, N. M., Jimenez, J. L., Kessler, S. H., Canagaratna, M. R., Wilson, K. R., Altieri, K. E., Mazzoleni, L. R., Wozniak, A. S., Bluhm, H., Mysak, E. R., Smith, J. D., Kolb, C. E., and Worsnop, D. R.: Carbon oxidation state as a metric for describing the chemistry of atmospheric organic aerosol, Nature Chem., 3, 133–139, https://doi.org/10.1038/nchem.948, 2011.

Landwehr, S., Volpi, M., Haumann, F. A., Robinson, C. M., Thurnherr, I., Ferracci, V., Baccarini, A., Thomas, J., Gorodetskaya, I., Tatzelt, C., Henning, S., Modini, R. L., Forrer, H. J., Lin, Y., Cassar, N., Simó, R., Hassler, C., Moallemi, A., Fawcett, S. E., Harris, N., Airs, R., Derkani, M. H., Alberello, A., Toffoli, A., Chen, G., Rodríguez-Ros, P., Zamanillo, M., Cortés-Greus, P., Xue, L., Bolas, C. G., Leonard, K. C., Perez-Cruz, F., Walton, D., and Schmale, J.: Exploring the coupled ocean and atmosphere system with a data science approach applied to observations from the Antarctic Circumnavigation Expedition, Earth Syst. Dynam., 12, 1295–1369, https://doi.org/10.5194/esd-12-1295-2021, 2021.

Laskin, A., Laskin, J., and Nizkorodov, S. A.: Mass spectrometric approaches for chemical characterisation of atmospheric aerosols: critical review of the most recent advances, Environ. Chem., 9, 163, https://doi.org/10.1071/EN12052, 2012.

Lawler, M. J., Schill, G. P., Brock, C. A., Froyd, K. D., Williamson, C., Kupc, A., and Murphy, D. M.: Sea Spray Aerosol Over the Remote Oceans Has Low Organic Content, AGU Advances, 5, e2024AV001215, https://doi.org/10.1029/2024AV001215, 2024.

Lee, H. D., Morris, H. S., Laskina, O., Sultana, C. M., Lee, C., Jayarathne, T., Cox, J. L., Wang, X., Hasenecz, E. S., DeMott, P. J., Bertram, T. H., Cappa, C. D., Stone, E. A., Prather, K. A., Grassian, V. H., and Tivanski, A. V.: Organic Enrichment, Physical Phase State, and Surface Tension Depression of Nascent Core–Shell Sea Spray Aerosols during Two Phytoplankton Blooms, ACS Earth Space Chem., 4, 650–660, https://doi.org/10.1021/acsearthspacechem.0c00032, 2020.

Lehahn, Y., Koren, I., Schatz, D., Frada, M., Sheyn, U., Boss, E., Efrati, S., Rudich, Y., Trainic, M., Sharoni, S., Laber, C., DiTullio, G. R., Coolen, M. J. L., Martins, A. M., Van Mooy, B. A. S., Bidle, K. D., and Vardi, A.: Decoupling Physical from Biological Processes to Assess the Impact of Viruses on a Mesoscale Algal Bloom, Curr. Biol., 24, 2041–2046, https://doi.org/10.1016/j.cub.2014.07.046, 2014.

Lewis, S. L., Saliba, G., Russell, L. M., Quinn, P. K., Bates, T. S., and Behrenfeld, M. J.: Seasonal Differences in Submicron Marine Aerosol Particle Organic Composition in the North Atlantic, Front. Mar. Sci., 8, 720208, https://doi.org/10.3389/fmars.2021.720208, 2021.

Li, Y., Bai, B., Dykema, J., Shin, N., Lambe, A. T., Chen, Q., Kuwata, M., Ng, N. L., Keutsch, F. N., and Liu, P.: Predicting Real Refractive Index of Organic Aerosols From Elemental Composition, Geophys. Res. Lett., 50, e2023GL103446, https://doi.org/10.1029/2023GL103446, 2023.

Lin, C., Ceburnis, D., Hellebust, S., Buckley, P., Wenger, J., Canonaco, F., Prévôt, A. S. H., Huang, R.-J., O'Dowd, C., and Ovadnevaite, J.: Characterization of Primary Organic Aerosol from Domestic Wood, Peat, and Coal Burning in Ireland, Environ. Sci. Technol., 51, 10624–10632, https://doi.org/10.1021/acs.est.7b01926, 2017.

Lin, C., Ceburnis, D., Huang, R.-J., Xu, W., Spohn, T., Martin, D., Buckley, P., Wenger, J., Hellebust, S., Rinaldi, M., Facchini, M. C., O'Dowd, C., and Ovadnevaite, J.: Wintertime aerosol dominated by solid-fuel-burning emissions across Ireland: insight into the spatial and chemical variation in submicron aerosol, Atmos. Chem. Phys., 19, 14091–14106, https://doi.org/10.5194/acp-19-14091-2019, 2019.

Liu, Y., Ma, C., and Sun, J.: Integrated FT-ICR MS and metabolome reveals diatom-derived organic matter by bacterial transformation under warming and acidification, iScience, 26, 106812, https://doi.org/10.1016/j.isci.2023.106812, 2023.

Loh, A., Kim, D., An, J. G., Choi, N., and Yim, U. H.: Chemical characterization of sub-micron aerosols over the East Sea (Sea of Japan), Sci. Total Environ., 856, 159173, https://doi.org/10.1016/j.scitotenv.2022.159173, 2023.

Loh, A., Kim, D., An, J. G., Choi, N., and Yim, U. H.: Characteristics of sub-micron aerosols in the Yellow Sea and its environmental implications, Mar. Pollut. Bull., 204, 116556, https://doi.org/10.1016/j.marpolbul.2024.116556, 2024.

Long, Y., Zhang, W., Sun, N., Zhu, P., Yan, J., and Yin, S.: Sequential Interaction of Biogenic Volatile Organic Compounds and SOAs in Urban Forests Revealed Using Toeplitz Inverse Covariance-Based Clustering and Causal Inference, Forests, 14, 1617, https://doi.org/10.3390/f14081617, 2023.

Mallet, M. D., D'Anna, B., Mème, A., Bove, M. C., Cassola, F., Pace, G., Desboeufs, K., Di Biagio, C., Doussin, J.-F., Maille, M., Massabò, D., Sciare, J., Zapf, P., di Sarra, A. G., and Formenti, P.: Summertime surface PM_1 aerosol composition and size by source region at the Lampedusa island in the central Mediterranean Sea, Atmos. Chem. Phys., 19, 11123–11142, https://doi.org/10.5194/acp-19-11123-2019, 2019.

Malloy, Q. G. J., Li Qi, Warren, B., Cocker III, D. R., Erupe, M. E., and Silva, P. J.: Secondary organic aerosol formation from primary aliphatic amines with NO_3 radical, Atmos. Chem. Phys., 9, 2051–2060, https://doi.org/10.5194/acp-9-2051-2009, 2009.

Mansour, K., Decesari, S., Facchini, M. C., Belosi, F., Paglione, M., Sandrini, S., Bellacicco, M., Marullo, S., Santoleri, R., Ovadnevaite, J., Ceburnis, D., O'Dowd, C., Roberts, G., Sanchez, K., and Rinaldi, M.: Linking Marine Biological Activity to Aerosol Chemical Composition and Cloud-Relevant Properties Over the North Atlantic Ocean, J. Geophys. Res.-Atmos., 125, e2019JD032246, https://doi.org/10.1029/2019JD032246, 2020.

Mansour, K., Decesari, S., Ceburnis, D., Ovadnevaite, J., and Rinaldi, M.: Machine learning for prediction of daily sea surface dimethylsulfide concentration and emission flux over the North Atlantic Ocean (1998–2021), Sci. Total Environ., 871, 162123, https://doi.org/10.1016/j.scitotenv.2023.162123, 2023.

Mansour, K., Decesari, S., Ceburnis, D., Ovadnevaite, J., Russell, L. M., Paglione, M., Poulain, L., Huang, S., O'Dowd, C., and Rinaldi, M.: IPB−MSA&SO_4 : a daily 0.25° resolution dataset of in situ-produced biogenic methanesulfonic acid and sulfate over the North Atlantic during 1998–2022 based on machine learning, Earth Syst. Sci. Data, 16, 2717–2740, https://doi.org/10.5194/essd-16-2717-2024, 2024.

Marais, E. A., Jacob, D. J., Jimenez, J. L., Campuzano-Jost, P., Day, D. A., Hu, W., Krechmer, J., Zhu, L., Kim, P. S., Miller, C. C., Fisher, J. A., Travis, K., Yu, K., Hanisco, T. F., Wolfe, G. M., Arkinson, H. L., Pye, H. O. T., Froyd, K. D., Liao, J., and McNeill, V. F.: Aqueous-phase mechanism for secondary organic aerosol formation from isoprene: application to the southeast United States and co-benefit of SO_2 emission controls, Atmos. Chem. Phys., 16, 1603–1618, https://doi.org/10.5194/acp-16-1603-2016, 2016.

Markuszewski, P., Nilsson, E. D., Zinke, J., Mårtensson, E. M., Salter, M., Makuch, P., Kitowska, M., Niedźwiecka-Wróbel, I., Drozdowska, V., Lis, D., Petelski, T., Ferrero, L., and Piskozub, J.: Multi-year gradient measurements of sea spray fluxes over the Baltic Sea and the North Atlantic Ocean, EGUsphere [preprint], https://doi.org/10.5194/egusphere-2024-1254, 2024.

Mayer, K. J., Wang, X., Santander, M. V., Mitts, B. A., Sauer, J. S., Sultana, C. M., Cappa, C. D., and Prather, K. A.: Secondary Marine Aerosol Plays a Dominant Role over Primary Sea Spray Aerosol in Cloud Formation, ACS Cent. Sci., 6, 2259–2266, https://doi.org/10.1021/acscentsci.0c00793, 2020.

Maykut, N. N., Lewtas, J., Kim, E., and Larson, T. V.: Source Apportionment of $PM_{2.5}$ at an Urban IMPROVE Site in Seattle, Washington, Environ. Sci. Technol., 37, 5135–5142, https://doi.org/10.1021/es030370y, 2003.

McNeill, V. F.: Aqueous Organic Chemistry in the Atmosphere: Sources and Chemical Processing of Organic Aerosols, Environ. Sci. Technol., 49, 1237–1244, https://doi.org/10.1021/es5043707, 2015.

Meador, T. B., Goldenstein, N. I., Gogou, A., Herut, B., Psarra, S., Tsagaraki, T. M., and Hinrichs, K.-U.: Planktonic Lipidome Responses to Aeolian Dust Input in Low-Biomass Oligotrophic Marine Mesocosms, Front. Mar. Sci., 4, 113, https://doi.org/10.3389/fmars.2017.00113, 2017.

Middlebrook, A. M., Bahreini, R., Jimenez, J. L., and Canagaratna, M. R.: Evaluation of Composition-Dependent Collection Efficiencies for the Aerodyne Aerosol Mass Spectrometer using Field Data, Aerosol Sci. Tech., 46, 258–271, https://doi.org/10.1080/02786826.2011.620041, 2012.

Miyazaki, Y., Sawano, M., and Kawamura, K.: Low-molecular-weight hydroxyacids in marine atmospheric aerosol: evidence of a marine microbial origin, Biogeosciences, 11, 4407–4414, https://doi.org/10.5194/bg-11-4407-2014, 2014.

Mohr, C., DeCarlo, P. F., Heringa, M. F., Chirico, R., Slowik, J. G., Richter, R., Reche, C., Alastuey, A., Querol, X., Seco, R., Peñuelas, J., Jiménez, J. L., Crippa, M., Zimmermann, R., Baltensperger, U., and Prévôt, A. S. H.: Identification and quantification of organic aerosol from cooking and other sources in Barcelona using aerosol mass spectrometer data, Atmos. Chem. Phys., 12, 1649–1665, https://doi.org/10.5194/acp-12-1649-2012, 2012.

Moschos, V., Dzepina, K., Bhattu, D., Lamkaddam, H., Casotto, R., Daellenbach, K. R., Canonaco, F., Rai, P., Aas, W., Becagli, S., Calzolai, G., Eleftheriadis, K., Moffett, C. E., Schnelle-Kreis, J., Severi, M., Sharma, S., Skov, H., Vestenius, M., Zhang, W., Hakola, H., Hellén, H., Huang, L., Jaffrezo, J.-L., Massling, A., Nøjgaard, J. K., Petäjä, T., Popovicheva, O., Sheesley, R. J., Traversi, R., Yttri, K. E., Schmale, J., Prévôt, A. S. H., Baltensperger, U., and El Haddad, I.: Equal abundance of summertime natural and wintertime anthropogenic Arctic organic aerosols, Nat. Geosci., 15, 196–202, https://doi.org/10.1038/s41561-021-00891-1, 2022.

Mungall, E. L., Wong, J. P. S., and Abbatt, J. P. D.: Heterogeneous Oxidation of Particulate Methanesulfonic Acid by the Hydroxyl Radical: Kinetics and Atmospheric Implications, ACS Earth Space Chem., 2, 48–55, https://doi.org/10.1021/acsearthspacechem.7b00114, 2018.

Mutshinda, C. M., Finkel, Z. V., and Irwin, A. J.: Large shifts in diatom and dinoflagellate biomass in the North Atlantic over six decades, bioRxiv, https://doi.org/10.1101/2024.07.02.601152, 2024.

Narayanaswamy, B. E., Renaud, P. E., Duineveld, G. C. A., Berge, J., Lavaleye, M. S. S., Reiss, H., and Brattegard, T.: Biodiversity Trends along the Western European Margin, PLoS ONE, 5, e14295, https://doi.org/10.1371/journal.pone.0014295, 2010.

Nault, B. A., Croteau, P., Jayne, J., Williams, A., Williams, L., Worsnop, D., Katz, E. F., DeCarlo, P. F., and Canagaratna, M.: Laboratory evaluation of organic aerosol relative ionization efficiencies in the aerodyne aerosol mass spectrometer and aerosol chemical speciation monitor, Aerosol Sci. Tech., 57, 981–997, https://doi.org/10.1080/02786826.2023.2223249, 2023.

Ng, N. L., Canagaratna, M. R., Jimenez, J. L., Chhabra, P. S., Seinfeld, J. H., and Worsnop, D. R.: Changes in organic aerosol composition with aging inferred from aerosol mass spectra, Atmos. Chem. Phys., 11, 6465–6474, https://doi.org/10.5194/acp-11-6465-2011, 2011.

Nielsen, I. E., Skov, H., Massling, A., Eriksson, A. C., Dall'Osto, M., Junninen, H., Sarnela, N., Lange, R., Collier, S., Zhang, Q., Cappa, C. D., and Nøjgaard, J. K.: Biogenic and anthropogenic sources of aerosols at the High Arctic site Villum Research Station, Atmos. Chem. Phys., 19, 10239–10256, https://doi.org/10.5194/acp-19-10239-2019, 2019.

Nøjgaard, J. K., Peker, L., Pernov, J. B., Johnson, M. S., Bossi, R., Massling, A., Lange, R., Nielsen, I. E., Prevot, A. S. H., Eriksson, A. C., Canonaco, F., and Skov, H.: A local marine source of atmospheric particles in the High Arctic, Atmos. Environ., 285, 119241, https://doi.org/10.1016/j.atmosenv.2022.119241, 2022.

Nursanto, F. R., Meinen, R., Holzinger, R., Krol, M. C., Liu, X., Dusek, U., Henzing, B., and Fry, J. L.: What chemical species are responsible for new particle formation and growth in the Netherlands? A hybrid positive matrix factorization (PMF) analysis using aerosol composition (ACSM) and size (SMPS), EGUsphere [preprint], https://doi.org/10.5194/egusphere-2023-554, 2023.

O'Dowd, C., Ceburnis, D., Ovadnevaite, J., Vaishya, A., Rinaldi, M., and Facchini, M. C.: Do anthropogenic, continental or coastal aerosol sources impact on a marine aerosol signature at Mace Head?, Atmos. Chem. Phys., 14, 10687–10704, https://doi.org/10.5194/acp-14-10687-2014, 2014.

O'Dowd, C., Ceburnis, D., Ovadnevaite, J., Bialek, J., Stengel, D. B., Zacharias, M., Nitschke, U., Connan, S., Rinaldi, M., Fuzzi, S., Decesari, S., Cristina Facchini, M., Marullo, S., Santoleri, R., Dell'Anno, A., Corinaldesi, C., Tangherlini, M., and Danovaro, R.: Connecting marine productivity to sea-spray via nanoscale biological processes: Phytoplankton Dance or Death Disco?, Sci. Rep., 5, 14883, https://doi.org/10.1038/srep14883, 2015.

O'Dowd, C. D., Facchini, M. C., Cavalli, F., Ceburnis, D., Mircea, M., Decesari, S., Fuzzi, S., Yoon, Y. J., and Putaud, J.-P.: Biogenically driven organic contribution to marine aerosol, Nature, 431, 676–680, https://doi.org/10.1038/nature02959, 2004.

Ovadnevaite, J., O'Dowd, C., Dall'Osto, M., Ceburnis, D., Worsnop, D. R., and Berresheim, H.: Detecting high contributions of primary organic matter to marine aerosol: A case study, Geophys. Res. Lett., 38, https://doi.org/10.1029/2010GL046083, 2011.

Ovadnevaite, J., Ceburnis, D., Canagaratna, M., Berresheim, H., Bialek, J., Martucci, G., Worsnop, D. R., and O'Dowd, C.: On the effect of wind speed on submicron sea salt mass concentrations and source fluxes, J. Geophys. Res., 117, https://doi.org/10.1029/2011JD017379, 2012.

Ovadnevaite, J., Ceburnis, D., Leinert, S., Dall'Osto, M., Canagaratna, M., O'Doherty, S., Berresheim, H., and O'Dowd, C.: Submicron NE Atlantic marine aerosol chemical composition and abundance: Seasonal trends and air mass categorization: Seasonal Trends of Marine Aerosol, J. Geophys. Res.-Atmos., 119, 11850–11863, https://doi.org/10.1002/2013JD021330, 2014.

Ovadnevaite, J., Zuend, A., Laaksonen, A., Sanchez, K. J., Roberts, G., Ceburnis, D., Decesari, S., Rinaldi, M., Hodas, N., Facchini, M. C., Seinfeld, J. H., and O' Dowd, C.: Surface tension prevails over solute effect in organic-influenced cloud droplet activation, Nature, 546, 637–641, https://doi.org/10.1038/nature22806, 2017.

Oziel, L., Baudena, A., Ardyna, M., Massicotte, P., Randelhoff, A., Sallée, J.-B., Ingvaldsen, R. B., Devred, E., and Babin, M.: Faster Atlantic currents drive poleward expansion of temperate phytoplankton in the Arctic Ocean, Nat. Commun., 11, 1705, https://doi.org/10.1038/s41467-020-15485-5, 2020.

Paatero, P.: The Multilinear Engine – A Table-Driven, Least Squares Program for Solving Multilinear Problems, Including the *n*-Way Parallel Factor Analysis Model, J. Comput. Graph. Stat., 8, 854–888, https://doi.org/10.1080/10618600.1999.10474853, 1999.

Paatero, P. and Tapper, U.: Positive matrix factorization: A non-negative factor model with optimal utilization of error estimates of data values, Environmetrics, 5, 111–126, https://doi.org/10.1002/env.3170050203, 1994.

Paglione, M., Beddows, D. C. S., Jones, A., Lachlan-Cope, T., Rinaldi, M., Decesari, S., Manarini, F., Russo, M., Mansour, K., Harrison, R. M., Mazzanti, A., Tagliavini, E., and Dall'Osto, M.: Simultaneous organic aerosol source apportionment at two Antarctic sites reveals large-scale and ecoregion-specific components, Atmos. Chem. Phys., 24, 6305–6322, https://doi.org/10.5194/acp-24-6305-2024, 2024.

Park, J., Jang, J., Yoon, Y. J., Kang, S., Kang, H., Park, K., Cho, K. H., Kim, J.-H., Dall'Osto, M., and Lee, B. Y.: When river water meets seawater: Insights into primary marine aerosol production, Sci. Total Environ., 807, 150866, https://doi.org/10.1016/j.scitotenv.2021.150866, 2022.

Peltola, M., Rose, C., Trueblood, J. V., Gray, S., Harvey, M., and Sellegri, K.: Chemical precursors of new particle formation in coastal New Zealand, Atmos. Chem. Phys., 23, 3955–3983, https://doi.org/10.5194/acp-23-3955-2023, 2023.

Pettersen, C., Henderson, S. A., Mattingly, K. S., Bennartz, R., and Breeden, M. L.: The Critical Role of Euro-Atlantic Blocking in Promoting Snowfall in Central Greenland, J. Geophys. Res.-Atmos., 127, e2021JD035776, https://doi.org/10.1029/2021JD035776, 2022.

Preece, J. R., Mote, T. L., Cohen, J., Wachowicz, L. J., Knox, J. A., Tedesco, M., and Kooperman, G. J.: Summer atmospheric circulation over Greenland in response to Arctic amplification and diminished spring snow cover, Nat. Commun., 14, 3759, https://doi.org/10.1038/s41467-023-39466-6, 2023.

Quinn, P. K., Coffman, D. J., Johnson, J. E., Upchurch, L. M., and Bates, T. S.: Small fraction of marine cloud condensation nuclei made up of sea spray aerosol, Nat. Geosci., 10, 674–679, https://doi.org/10.1038/ngeo3003, 2017.

Rahmstorf, S., Box, J. E., Feulner, G., Mann, M. E., Robinson, A., Rutherford, S., and Schaffernicht, E. J.: Exceptional twentieth-century slowdown in Atlantic Ocean overturning circulation, Nat. Clim. Change, 5, 475–480, https://doi.org/10.1038/nclimate2554, 2015.

Rapf, R. J., Dooley, M. R., Kappes, K., Perkins, R. J., and Vaida, V.: pH Dependence of the Aqueous Photochem-

istry of α-Keto Acids, J. Phys. Chem. A, 121, 8368–8379, https://doi.org/10.1021/acs.jpca.7b08192, 2017.

Rinaldi, M., Fuzzi, S., Decesari, S., Marullo, S., Santoleri, R., Provenzale, A., Von Hardenberg, J., Ceburnis, D., Vaishya, A., O'Dowd, C. D., and Facchini, M. C.: Is chlorophyll-*a* the best surrogate for organic matter enrichment in submicron primary marine aerosol?, J. Geophys. Res.-Atmos., 118, 4964–4973, https://doi.org/10.1002/jgrd.50417, 2013.

Rinaldi, M., Paglione, M., Decesari, S., Harrison, R. M., Beddows, D. C. S., Ovadnevaite, J., Ceburnis, D., O'Dowd, C. D., Simó, R., and Dall'Osto, M.: Contribution of Water-Soluble Organic Matter from Multiple Marine Geographic Eco-Regions to Aerosols around Antarctica, Environ. Sci. Technol., 54, 7807–7817, https://doi.org/10.1021/acs.est.0c00695, 2020.

Robinson, N. H., Hamilton, J. F., Allan, J. D., Langford, B., Oram, D. E., Chen, Q., Docherty, K., Farmer, D. K., Jimenez, J. L., Ward, M. W., Hewitt, C. N., Barley, M. H., Jenkin, M. E., Rickard, A. R., Martin, S. T., McFiggans, G., and Coe, H.: Evidence for a significant proportion of Secondary Organic Aerosol from isoprene above a maritime tropical forest, Atmos. Chem. Phys., 11, 1039–1050, https://doi.org/10.5194/acp-11-1039-2011, 2011.

Rosenfeld, D., Zhu, Y., Wang, M., Zheng, Y., Goren, T., and Yu, S.: Aerosol-driven droplet concentrations dominate coverage and water of oceanic low-level clouds, Science, 363, eaav0566, https://doi.org/10.1126/science.aav0566, 2019.

Rousseaux, C. S., Hirata, T., and Gregg, W. W.: Satellite views of global phytoplankton community distributions using an empirical algorithm and a numerical model, Biogeosciences Discuss., 10, 1083–1109, https://doi.org/10.5194/bgd-10-1083-2013, 2013.

Russell, L. M., Bahadur, R., and Ziemann, P. J.: Identifying organic aerosol sources by comparing functional group composition in chamber and atmospheric particles, P. Natl. Acad. Sci. USA, 108, 3516–3521, https://doi.org/10.1073/pnas.1006461108, 2011.

Saha, M. and Fink, P.: Algal volatiles – the overlooked chemical language of aquatic primary producers, Biol. Rev., 97, 2162–2173, https://doi.org/10.1111/brv.12887, 2022.

Saliba, G., Chen, C.-L., Lewis, S., Russell, L. M., Rivellini, L.-H., Lee, A. K. Y., Quinn, P. K., Bates, T. S., Haëntjens, N., Boss, E. S., Karp-Boss, L., Baetge, N., Carlson, C. A., and Behrenfeld, M. J.: Factors driving the seasonal and hourly variability of sea-spray aerosol number in the North Atlantic, P. Natl. Acad. Sci. USA, 116, 20309–20314, https://doi.org/10.1073/pnas.1907574116, 2019.

Sanchez, K. J., Zhang, B., Liu, H., Brown, M. D., Crosbie, E. C., Gallo, F., Hair, J. W., Hostetler, C. A., Jordan, C. E., Robinson, C. E., Scarino, A. J., Shingler, T. J., Shook, M. A., Thornhill, K. L., Wiggins, E. B., Winstead, E. L., Ziemba, L. D., Saliba, G., Lewis, S. L., Russell, L. M., Quinn, P. K., Bates, T. S., Porter, J., Bell, T. G., Gaube, P., Saltzman, E. S., Behrenfeld, M. J., and Moore, R. H.: North Atlantic Ocean SST-gradient-driven variations in aerosol and cloud evolution along Lagrangian cold-air outbreak trajectories, Atmos. Chem. Phys., 22, 2795–2815, https://doi.org/10.5194/acp-22-2795-2022, 2022.

Sanders, R. N. C., Jones, D. C., Josey, S. A., Sinha, B., and Forget, G.: Causes of the 2015 North Atlantic cold anomaly in a global state estimate, Ocean Sci., 18, 953–978, https://doi.org/10.5194/os-18-953-2022, 2022.

Schmale, J., Schneider, J., Nemitz, E., Tang, Y. S., Dragosits, U., Blackall, T. D., Trathan, P. N., Phillips, G. J., Sutton, M., and Braban, C. F.: Sub-Antarctic marine aerosol: dominant contributions from biogenic sources, Atmos. Chem. Phys., 13, 8669–8694, https://doi.org/10.5194/acp-13-8669-2013, 2013.

Schneider, J., Freutel, F., Zorn, S. R., Chen, Q., Farmer, D. K., Jimenez, J. L., Martin, S. T., Artaxo, P., Wiedensohler, A., and Borrmann, S.: Mass-spectrometric identification of primary biological particle markers and application to pristine submicron aerosol measurements in Amazonia, Atmos. Chem. Phys., 11, 11415–11429, https://doi.org/10.5194/acp-11-11415-2011, 2011.

Schreiber, T.: Measuring Information Transfer, Phys. Rev. Lett., 85, 461–464, https://doi.org/10.1103/PhysRevLett.85.461, 2000.

Seidel, M., Vemulapalli, S. P. B., Mathieu, D., and Dittmar, T.: Marine Dissolved Organic Matter Shares Thousands of Molecular Formulae Yet Differs Structurally across Major Water Masses, Environ. Sci. Technol., 56, 3758–3769, https://doi.org/10.1021/acs.est.1c04566, 2022.

Sellegri, K., Nicosia, A., Freney, E., Uitz, J., Thyssen, M., Grégori, G., Engel, A., Zäncker, B., Haëntjens, N., Mas, S., Picard, D., Saint-Macary, A., Peltola, M., Rose, C., Trueblood, J., Lefevre, D., D'Anna, B., Desboeufs, K., Meskhidze, N., Guieu, C., and Law, C. S.: Surface ocean microbiota determine cloud precursors, Sci. Rep., 11, 281, https://doi.org/10.1038/s41598-020-78097-5, 2021.

Sellegri, K., Harvey, M., Peltola, M., Saint-Macary, A., Barthelmeß, T., Rocco, M., Moore, K. A., Cristi, A., Peyrin, F., Barr, N., Labonnote, L., Marriner, A., McGregor, J., Safi, K., Deppeler, S., Archer, S., Dunne, E., Harnwell, J., Delanoe, J., Freney, E., Rose, C., Bazantay, C., Planche, C., Saiz-Lopez, A., Quintanilla-López, J. E., Lebrón-Aguilar, R., Rinaldi, M., Banson, S., Joseph, R., Lupascu, A., Jourdan, O., Mioche, G., Colomb, A., Olivares, G., Querel, R., McDonald, A., Plank, G., Bukosa, B., Dillon, W., Pelon, J., Baray, J.-L., Tridon, F., Donnadieu, F., Szczap, F., Engel, A., DeMott, P. J., and Law, C. S.: Sea2Cloud: From Biogenic Emission Fluxes to Cloud Properties in the Southwest Pacific, B. Am. Meteorol. Soc., 104, E1017–E1043, https://doi.org/10.1175/BAMS-D-21-0063.1, 2023.

Semper, S., Våge, K., Pickart, R. S., Jónsson, S., and Valdimarsson, H.: Evolution and Transformation of the North Icelandic Irminger Current Along the North Iceland Shelf, J. Geophys. Res.-Oceans, 127, e2021JC017700, https://doi.org/10.1029/2021JC017700, 2022.

Simon, H., Bhave, P. V., Swall, J. L., Frank, N. H., and Malm, W. C.: Determining the spatial and seasonal variability in OM/OC ratios across the US using multiple regression, Atmos. Chem. Phys., 11, 2933–2949, https://doi.org/10.5194/acp-11-2933-2011, 2011.

Sinha, S., Sharma, H., and Shrivastava, M.: Application of advanced causal analyses to identify processes governing secondary organic aerosols, Sci. Rep., 14, 10718, https://doi.org/10.1038/s41598-024-59887-7, 2024.

Slowik, J. G., Vlasenko, A., McGuire, M., Evans, G. J., and Abbatt, J. P. D.: Simultaneous factor analysis of organic particle and gas mass spectra: AMS and PTR-MS measurements at an urban site, Atmos. Chem. Phys., 10, 1969–1988, https://doi.org/10.5194/acp-10-1969-2010, 2010.

Stein, A. F., Draxler, R. R., Rolph, G. D., Stunder, B. J. B., Cohen, M. D., and Ngan, F.: NOAA's HYSPLIT Atmospheric Transport and Dispersion Modeling System, B. Am. Meteorol. Soc., 96, 2059–2077, https://doi.org/10.1175/BAMS-D-14-00110.1, 2015.

Tong, Y., Qi, L., Stefenelli, G., Wang, D. S., Canonaco, F., Baltensperger, U., Prévôt, A. S. H., and Slowik, J. G.: Quantification of primary and secondary organic aerosol sources by combined factor analysis of extractive electrospray ionisation and aerosol mass spectrometer measurements (EESI-TOF and AMS), Atmos. Meas. Tech., 15, 7265–7291, https://doi.org/10.5194/amt-15-7265-2022, 2022.

Ulbrich, I. M., Canagaratna, M. R., Zhang, Q., Worsnop, D. R., and Jimenez, J. L.: Interpretation of organic components from Positive Matrix Factorization of aerosol mass spectrometric data, Atmos. Chem. Phys., 9, 2891–2918, https://doi.org/10.5194/acp-9-2891-2009, 2009.

Van Alstyne, K. and Houser, L.: Dimethylsulfide release during macroinvertebrate grazing and its role as an activated chemical defense, Mar. Ecol. Prog. Ser., 250, 175–181, https://doi.org/10.3354/meps250175, 2003.

van Pinxteren, M., Robinson, T.-B., Zeppenfeld, S., Gong, X., Bahlmann, E., Fomba, K. W., Triesch, N., Stratmann, F., Wurl, O., Engel, A., Wex, H., and Herrmann, H.: High number concentrations of transparent exopolymer particles in ambient aerosol particles and cloud water – a case study at the tropical Atlantic Ocean, Atmos. Chem. Phys., 22, 5725–5742, https://doi.org/10.5194/acp-22-5725-2022, 2022.

Veron, F.: Ocean Spray, Annu. Rev. Fluid Mech., 47, 507–538, https://doi.org/10.1146/annurev-fluid-010814-014651, 2015.

Villermaux, E., Wang, X., and Deike, L.: Bubbles spray aerosols: Certitudes and mysteries, PNAS Nexus, 1, pgac261, https://doi.org/10.1093/pnasnexus/pgac261, 2022.

Wang, Y., Zheng, X., Dong, X., Xi, B., Wu, P., Logan, T., and Yung, Y. L.: Impacts of long-range transport of aerosols on marine-boundary-layer clouds in the eastern North Atlantic, Atmos. Chem. Phys., 20, 14741–14755, https://doi.org/10.5194/acp-20-14741-2020, 2020.

Willis, M. D., Köllner, F., Burkart, J., Bozem, H., Thomas, J. L., Schneider, J., Aliabadi, A. A., Hoor, P. M., Schulz, H., Herber, A. B., Leaitch, W. R., and Abbatt, J. P. D.: Evidence for marine biogenic influence on summertime Arctic aerosol, Geophys. Res. Lett., 44, 6460–6470, https://doi.org/10.1002/2017GL073359, 2017.

Willoughby, A., Wozniak, A., and Hatcher, P.: Detailed Source-Specific Molecular Composition of Ambient Aerosol Organic Matter Using Ultrahigh Resolution Mass Spectrometry and 1H NMR, Atmosphere, 7, 79, https://doi.org/10.3390/atmos7060079, 2016.

Wolf, K. K. E., Hoppe, C. J. M., Rehder, L., Schaum, E., John, U., and Rost, B.: Heatwave responses of Arctic phytoplankton communities are driven by combined impacts of warming and cooling, Sci. Adv., 10, eadl5904, https://doi.org/10.1126/sciadv.adl5904, 2024.

Xu, W., Lambe, A., Silva, P., Hu, W., Onasch, T., Williams, L., Croteau, P., Zhang, X., Renbaum-Wolff, L., Fortner, E., Jimenez, J. L., Jayne, J., Worsnop, D., and Canagaratna, M.: Laboratory evaluation of species-dependent relative ionization efficiencies in the Aerodyne Aerosol Mass Spectrometer, Aerosol Sci. Technol., 52, 626–641, https://doi.org/10.1080/02786826.2018.1439570, 2018.

Xu, W., Ovadnevaite, J., Fossum, K. N., Lin, C., Huang, R.-J., O'Dowd, C., and Ceburnis, D.: Aerosol hygroscopicity and its link to chemical composition in the coastal atmosphere of Mace Head: marine and continental air masses, Atmos. Chem. Phys., 20, 3777–3791, https://doi.org/10.5194/acp-20-3777-2020, 2020.

Xu, W., Fossum, K. N., Ovadnevaite, J., Lin, C., Huang, R.-J., O'Dowd, C., and Ceburnis, D.: The impact of aerosol size-dependent hygroscopicity and mixing state on the cloud condensation nuclei potential over the north-east Atlantic, Atmos. Chem. Phys., 21, 8655–8675, https://doi.org/10.5194/acp-21-8655-2021, 2021.

Yazdani, A., Dudani, N., Takahama, S., Bertrand, A., Prévôt, A. S. H., El Haddad, I., and Dillner, A. M.: Fragment ion–functional group relationships in organic aerosols using aerosol mass spectrometry and mid-infrared spectroscopy, Atmos. Meas. Tech., 15, 2857–2874, https://doi.org/10.5194/amt-15-2857-2022, 2022.

Zeppenfeld, S., van Pinxteren, M., Hartmann, M., Zeising, M., Bracher, A., and Herrmann, H.: Marine Carbohydrates in Arctic Aerosol Particles and Fog – Diversity of Oceanic Sources and Atmospheric Transformations, EGUsphere [preprint], https://doi.org/10.5194/egusphere-2023-1607, 2023.

Zhang, Q., Jimenez, J. L., Canagaratna, M. R., Ulbrich, I. M., Ng, N. L., Worsnop, D. R., and Sun, Y.: Understanding atmospheric organic aerosols via factor analysis of aerosol mass spectrometry: a review, Anal. Bioanal. Chem., 401, 3045–3067, https://doi.org/10.1007/s00216-011-5355-y, 2011.

Zhao, Z., He, Q., Lu, Z., Zhao, Q., and Wang, J.: Analysis of Atmospheric CO_2 and CO at Akedala Atmospheric Background Observation Station, a Regional Station in Northwestern China, Int. J. Env. Res. Pub. He., 19, 6948, https://doi.org/10.3390/ijerph19116948, 2022.

Zheng, G., Wang, Y., Wood, R., Jensen, M. P., Kuang, C., McCoy, I. L., Matthews, A., Mei, F., Tomlinson, J. M., Shilling, J. E., Zawadowicz, M. A., Crosbie, E., Moore, R., Ziemba, L., Andreae, M. O., and Wang, J.: New particle formation in the remote marine boundary layer, Nat. Commun., 12, 527, https://doi.org/10.1038/s41467-020-20773-1, 2021.